

RESEARCH ARTICLE

Function of the *Drosophila* receptor guanylyl cyclase Gyc76C in PlexA-mediated motor axon guidance

Kayam Chak and Alex L. Kolodkin*

ABSTRACT

The second messengers cAMP and cGMP modulate attraction and repulsion mediated by neuronal guidance cues. We find that the *Drosophila* receptor guanylyl cyclase Gyc76C genetically interacts with *Semaphorin 1a* (*Sema-1a*) and physically associates with the *Sema-1a* receptor plexin A (PlexA). PlexA regulates Gyc76C catalytic activity *in vitro*, and each distinct Gyc76C protein domain is crucial for regulating Gyc76C activity *in vitro* and motor axon guidance *in vivo*. The cytosolic protein dGIPC interacts with Gyc76C and facilitates *Sema-1a*-PlexA/Gyc76C-mediated motor axon guidance. These findings provide an *in vivo* link between semaphorin-mediated repulsive axon guidance and alteration of intracellular neuronal cGMP levels.

KEY WORDS: Receptor guanylyl cyclase, Gyc76C, cGMP, Semaphorin-1a, Plexin A, dGIPC, Axon guidance

INTRODUCTION

Both membrane-associated and secreted neuronal guidance cues can attract or repel axons and dendrites during neural development, and several families of guidance cues and receptors perform these functions (Dickson, 2002; Kolodkin and Tessier-Lavigne, 2011). Modulation of guidance cue activities through intracellular signaling components determines how extrinsic factors are interpreted by extending neuronal processes during development (Bashaw and Klein, 2010). For example, growth cone turning experiments *in vitro* demonstrate that attraction mediated by the guidance cue netrin-1 can be converted to repulsion by lowering intracellular cAMP (Ming et al., 1997), whereas repulsion mediated by the guidance cue Semaphorin 3A (*Sema-3A*) can be converted to attraction by increasing intracellular cGMP (Song et al., 1998). Elevated cAMP in cultured DRG neurons neutralizes *Sema-3A* growth cone collapse, whereas elevated cGMP potentiates it (Dontchev and Letourneau, 2002). The ratio of cAMP to cGMP can determine the sign of a growth cone steering response (Nishiyama et al., 2003), and *Sema-3A* induces cGMP production in neuronal growth cones, activating of cGMP-gated calcium channels (CNGCs), Ca^{2+} influx and repulsion (Togashi et al., 2008). cAMP and cGMP regulate kinases and phosphodiesterases to direct formation of axons or dendrites in cultured hippocampal neurons (Shelly et al., 2010). Therefore, coordination of cAMP and cGMP signaling regulates cellular responses to different stimuli in the neurons.

Guanylyl cyclases (GCs) include soluble and transmembrane proteins that catalyze the conversion of GTP to cGMP, and they

regulate a wide range of diverse cellular and physiological processes (Davies, 2006), including axonal and dendritic guidance (Polleux et al., 2000; Seidel and Bicker, 2000; Gibbs et al., 2001; Nishiyama et al., 2003). The mammalian receptor guanylyl cyclase GC-B and cGMP-dependent kinase I (cGKI) are essential for proper sensory axon afferent guidance into the CNS, and C-type natriuretic peptide is the GC-B ligand that is crucial for murine sensory axon branching, axon outgrowth and axon attraction (Schmidt et al., 2009; Zhao and Ma, 2009). Yet, how GCs are linked to axon guidance signaling to alter intracellular cGMP levels and modulate growth cone responses *in vivo* is unclear.

The *Drosophila* transmembrane semaphorin *Sema-1a* binds to the plexin A (PlexA) receptor to mediate axon-axon repulsion and to control axonal fasciculation in embryonic central and peripheral nervous systems (CNS and PNS) (Winberg et al., 1998b; Yu et al., 1998). The *Drosophila* receptor GC Gyc76C is required in motoneurons for *Sema-1a*-PlexA-mediated axon guidance and is dependent on the integrity of the Gyc76C catalytic cyclase domain (Ayoob et al., 2004). Here, we investigate connections between Gyc76C and *Sema-1a*-PlexA-mediated axon guidance. Our findings support the theory that Gyc76C-generated cGMP within neuronal growth cones facilitates axonal repulsion mediated by *Sema-1a* and PlexA, allowing for the establishment of *Drosophila* embryonic neuromuscular connectivity.

RESULTS**Gyc76C suppresses *Sema 1a*-mediated motor axon repulsion**

Gyc76C mutations act as dominant enhancers of a *Sema-1a*-dependent gain-of-function phenotype that affects CNS commissural axon midline crossing in *Drosophila* embryos (embryos with this genotype are referred to as '*PUP*' for the genetic elements in this background) (Ayoob et al., 2004). Altering Gyc76C gene dose modifies a PlexA-dependent gain-of-function phenotype in CNS longitudinal connective axons. Further, Gyc76C mutant embryos exhibit motor axon guidance defects similar to *Sema-1a* mutant embryos, and Gyc76C genetically interacts with *Sema-1a* and PlexA (Ayoob et al., 2004). These data suggest Gyc76C functions in *Sema-1a*-PlexA-mediated motor axon guidance. However, the *PUP* phenotypes are observed in a *Sema-1a*-null genetic background in which *Sema-1a* is ectopically expressed on CNS midline glia. However, the Gyc76C gain- and loss-of-function phenotypes observed previously in motor axons (Ayoob et al., 2004) do not allow for unequivocal assessments of responses to *Sema-1a* *in trans* independent of roles *Sema-1a* and Gyc76C might play in axon-axon interactions. Therefore, we employed a different *Sema-1a* gain-of-function paradigm to investigate Gyc76C-mediated repulsive signaling in motor axons in response to *Sema-1a* ligand presented *in trans*.

Sema-1a is enriched in *Drosophila* embryonic neurons and mediates axonal repulsion, ensuring proper axon pathfinding (Winberg et al., 1998b; Yu et al., 1998; Ayoob et al., 2004; Cho et

The Solomon H. Snyder Department of Neuroscience, Howard Hughes Medical Institute, The Johns Hopkins University School of Medicine, Baltimore, MD 21205, USA.

*Author for correspondence (kolodkin@jhmi.edu)

Received 26 February 2013; Accepted 26 September 2013

al., 2012; Jeong et al., 2012). During neural development, motor axons exit the CNS in two large bundles that include multiple motor axons which then segregate into smaller motor nerves: the intersegmental nerves (ISNs: ISNb and ISNd) and the segmental nerves (SNs: SNa and SNc) (Landgraf et al., 1997). The fasciclin II antibody 1D4 labels all motor axons, revealing stereotypic embryonic neuromuscular connectivity (Grenningloh et al., 1991; Van Vactor et al., 1993). ISNb axons defasciculate from the main ISN bundle and navigate along ventral longitudinal muscles, including muscles 6, 7, 12 and 13, to innervate appropriate targets (Van Vactor et al., 1993; Landgraf et al., 1997). At each choice point, the ISNb bundle extends nascent projections anteriorly and posteriorly between muscles, establishing initial presynaptic contacts with target muscles (i.e. RP3 and RP5 motor axons leave the ISNb, then innervate muscles 6 and 7, and muscles 12 and 13, respectively) (Fig. 1A).

We ectopically expressed Sema-1a in all embryonic muscles using the *Mef2-Gal4* driver (Ranganayakulu et al., 1996). Since Sema-1a is a motor axon repellent (Winberg et al., 1998a; Winberg et al., 1998b; Yu et al., 1998; Yu et al., 2000), we anticipated that Sema-1a-expressing muscles would influence ISNb axons (Fig. 1A, red circles). Removal of a signaling component involved in Sema-1a-mediated axon guidance should suppress, or enhance, gain-of-function phenotypes resulting from muscle-derived Sema-1a. We confirmed muscle expression of Sema-1a in both *UAS:Sema-1a/+*, *Mef2-Gal4/+* embryos (Fig. 1B) and *UAS:Sema-1a/+*, *Mef2-Gal4/+*; *Gyc76C^{ex173/+}* embryos (K.C. and A.L.K., unpublished) at embryonic stage 16 by immunohistochemistry with anti-Sema-1a (Yu et al., 1998). We observed a range of ISNb stalling and axon pathfinding defects categorized into five distinct phenotypes (see Table 1): (1) aberrant projection onto muscle 12 (M12); (2) stalling between

muscles 12 and 13 with no accompanying arborization (M12/13); (3) stalling at muscle 13, or between muscles 13 and 6 (M13, M13/6); (4) no presynaptic arborizations between muscles 6 and 7 (M6/7); and (5) distinct ISNb defects, including bypasses (BPs) and also axon-positioning defects (PDs). *UAS:Sema-1a/+*, *Mef2-Gal4/+* embryos exhibited ISNb defects in 54.0% of hemisegments; the majority of these defects were ISNb axon bundles stalled between muscles 12 and 13 (25.8%) (Table 1). Axon pathfinding defects, including those at M13 and M13/6 or at M6/7, were observed in 7.0% and 9.4% of hemisegments, respectively (Table 1). A significant number of ISNb BPs (8.0% of hemisegments) and PDs (8.4% of hemisegments) were observed in this *Sema-1a* gain-of-function paradigm (Fig. 1C, open arrowheads). ISNb BP events, including fusion and parallel bypasses, indicate a failure of the ISNb to innervate the entire ventral muscle field, resulting in ISNb dorsal extension along, or directly adjacent to, the ISN (Lin et al., 1994; Desai et al., 1996; Yu et al., 1998; Wills et al., 1999). The observed PDs are distinct ISNb pathfinding defects where the ISNb bundle does not deviate from the ISN bundle but RP3 or RP5 neurons still innervate target ventral muscles (Fig. 1C: open arrowhead, BP; asterisk, muscle innervation). Therefore, Sema-1a presented *in trans* on muscles acts as a motor axon repellent.

Removing one copy of *Gyc76C* produced significant reductions in total ISNb defects (Fig. 1C', open arrows), from 54.0% to 29.5% (Fig. 1D; Table 1; $P < 0.005$). Furthermore, both BPs and PDs were suppressed: from 8% to 1.2%, and from 8.4% to 3.2%, respectively, in *UAS:Sema-1a/+*, *Mef2-Gal4/+*; *Gyc76C^{ex173/+}* embryos. We observed similar suppression of these same phenotypes when one copy of *PlexA* was removed in this gain-of-function paradigm (*UAS:Sema-1a/+*, *Mef2-Gal4/+*; *PlexA^{Df(4)C3/+}*) (Fig. 1D and Table 1). Furthermore, *UAS:Sema-1a/+*; *Gyc76C^{ex173/+}* embryos

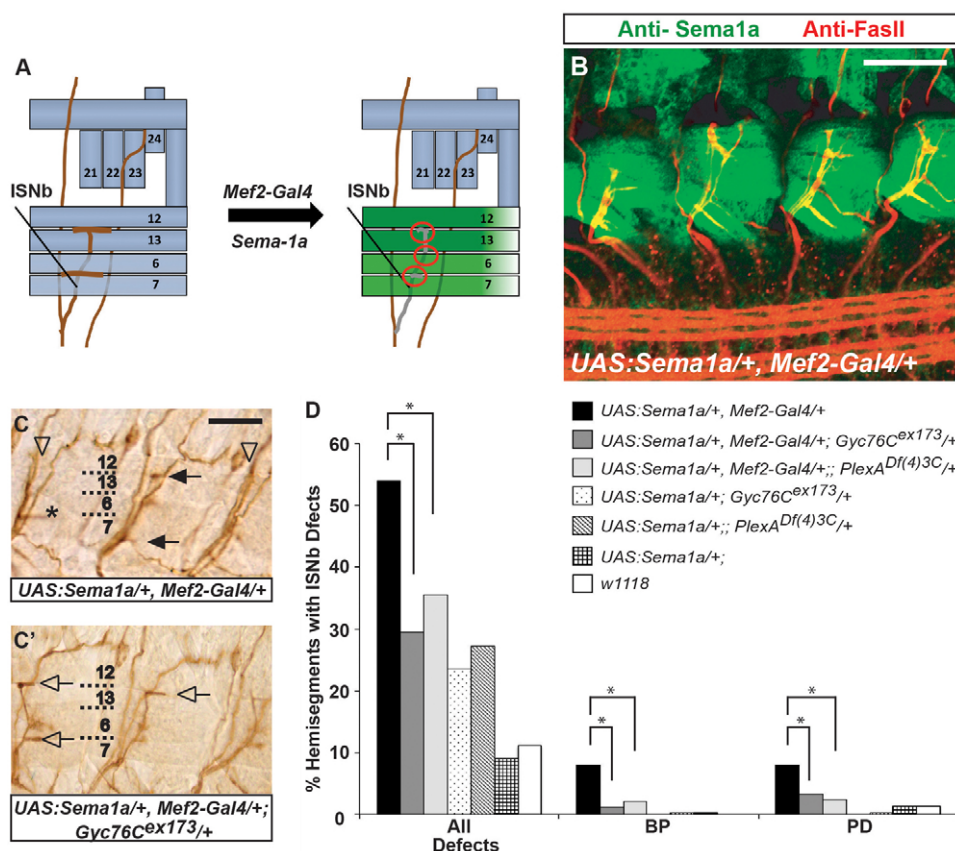


Fig. 1. *Gyc76C* suppresses Sema-1a-mediated repulsion of motor axons in the peripheral nervous system. (A) Schematic diagram of wild-type (left) and *Sema-1a* muscle gain-of-function (right) *Drosophila* embryonic hemisegments showing ISNb phenotypes (red circles). Anterior is leftwards; dorsal is upwards. (B) Filled stage 16 *Drosophila* embryo harboring *UAS:Sema1a/+*, *Mef2-GAL4/+* transgenes stained with the anti-fasciclin II (1D4, red) and anti-Sema-1a (green). Scale bar: 10 μ m. (C,C') Three hemisegments of late stage 16 embryos stained with 1D4. (C) In *UAS:Sema-1a/+*, *Mef2-GAL4/+* embryo, ISNb motor axons often fail to reach their ventral muscle targets (black arrows) or exhibit pathfinding defects (open arrowheads), including ISNb bypasses (BPs) and positioning defects (PDs, asterisk; see text). (C') In *UAS:Sema1a/+*, *Mef2-GAL4/+*; *Gyc76C^{ex173/+}* embryos, *Sema-1a* gain-of-function ISNb stalling phenotypes are greatly suppressed (open arrows). Scale bar: 5 μ m. (D) Quantification of total ISNb pathfinding defects, PBs and PDs following Sema-1a overexpression in muscles. Z-test for two proportions defines significant differences between genotypes; * $P < 0.005$ (see Table 1 for n values).

Table 1. ISNb defect phenotypes in *Sema-1a* GOF in different genetic backgrounds

	Total defects (n)*	M12	M12/13	M13, M13/6	M6/7	Distinct ISNb defects	
						Bypass [‡]	Positioning defect [§]
<i>UAS:Sema1a/+; Mef2-Gal4/+</i>	54.0% (287)	0.7%	25.8%	7.0%	9.4%	8.0%	8.4%
<i>UAS:Sema1a/+; Mef2-Gal4/+; Gyc76C^{ex173}/+</i>	29.5% (342) [¶]	0.3%	16.7%	5.3%	5.6%	1.2%	3.2%
<i>UAS:Sema1a/+; Mef2-Gal4/+;; PlexA^{Df(4)3}/+</i>	35.5% (344) [¶]	1.2%	16.0%	8.4%	7.8%	2.0%	2.3%
<i>UAS:Sema1; Gyc76C^{ex173}/+</i>	23.6% (343) [¶]	0.3%	17.2%	0%	7.6%	0%	0%
<i>UAS:Sema1a/+;; PlexA^{Df(4)3}/+</i>	27.1% (317) [¶]	0%	20.2%	1.9%	6.3%	0.3%	0.3%
<i>UAS:Sema1a/+</i>	9.1% (307)	0%	5.9%	0%	1.6%	0.3%	1.3%
<i>W1118</i>	11.1% (297)	0%	8.8%	0%	1.0%	0%	1.3%

*n=total number of hemisegments scored. Abnormal ISNb stalling phenotypes are defined as a failure of ISNb axons to innervate ventral lateral muscles (between 12/13 or 6/7). Phenotypes include weak, or absent, innervation between muscles 12/13 and between muscles 6/7, muscle target bypasses and axon positioning defects.

[‡]Bypass phenotypes, including parallel bypass and fusion bypass events, are defined as failure of ISNb axons to enter the ventral muscle field and extend dorsally in close proximity to the ISN or along the ISN, resulting in a thicker ISN bundle.

[§]Positioning defects are defined as ISNb axon bundles growing dorsally along the ISN but with RP3 or RP5 still innervating ventral muscles.

[¶]Significantly different from values for *UAS:Sema-1a/+; Mef2-Gal4/+* embryos. Z-test for two proportions; *P*<0.005.

exhibit a higher penetrance of motor axon defects than *UAS:Sema-1a/+* embryos (Fig. 1D and Table 1), indicating the presence of a modest dominant phenotype resulting from heterozygosity at *Gyc76C^{ex173}*. The strong suppression of *Sema-1a* gain-of-function motor axon phenotypes by removing one *Gyc76C* or *PlexA* allele suggests *Gyc76C* participates in *Sema-1a*-*PlexA*-mediated repulsive guidance *in vivo*.

Gyc76C physically associates with PlexA both *in vitro* and *in vivo*

We next performed co-immunoprecipitation (co-IP) experiments *in vitro* using a *Drosophila* embryonic cell line, and *in vivo* using transgenic fly lines. Myc-tagged full-length (FL) *Gyc76C* (Myc-FL *Gyc76C*) and/or hemagglutinin (HA)-tagged FL *PlexA* (HA-FL *PlexA*) were overexpressed in the adherent *Drosophila* S2R+ cell line (Schneider, 1972). Immunoprecipitation of Myc-FL *Gyc76C* using anti-Myc robustly co-immunoprecipitated HA-FL *PlexA* (Fig. 2A, lane 1). Immunoprecipitation of HA-FL *PlexA* using anti-HA precipitated Myc-FL *Gyc76C* (Fig. 2B, lane 3), and HA-FL *PlexA* or Myc-FL *Gyc76C* was not immunoprecipitated by anti-Myc or anti-HA, respectively (Fig. 2A, lane 3 and Fig. 2B, lane 2). We did not detect interactions between HA-FL *PlexA* and Myc-tagged dumbfounded (*Duf*), an immunoglobulin domain transmembrane protein required for muscle fusion (Ruiz-Gómez et al., 2000), in S2R+ cells (Fig. 2A, lane 5 and Fig. 2B, lane 5), demonstrating specificity in our immunoprecipitation experiments. We generated transgenic flies expressing HA-FL *PlexA* with, or without, Myc-FL *Gyc76C* in all neurons using the UAS-GAL4 system (Brand and Perrimon, 1993) and the neuronal driver *elav-Gal4*. Using anti-Myc or anti-HA, we confirmed the expression of each transgene in developing embryos (supplementary material Fig. S1). In embryonic lysates generated from these transgenic flies, we observed robust co-IP of Myc-FL *Gyc76C* using anti-HA (Fig. 2C, lane 2) only in flies expressing both HA-FL *PlexA* and Myc-FL *Gyc76C*. Therefore, *Gyc76C* and *PlexA* can form a protein complex both *in vitro* and *in vivo*.

To define region(s) of *Gyc76C* and *PlexA* that mediate association between these proteins, we generated three truncated HA-*PlexA* constructs: the *PlexA* extracellular region with transmembrane domain (HA-*PlexA* Ecto_{TM}), the *PlexA* intracellular region with transmembrane domain (HA-*PlexA* Endo_{TM}) and the *PlexA* intracellular region without transmembrane domain (HA-*PlexA*

Endo). Each truncated *PlexA* construct was expressed with, or without, Myc-FL *Gyc76C* in S2R+ cells. Myc-FL *Gyc76C* immunoprecipitated each of these HA-*PlexA* constructs (Fig. 2D, lanes 5-8). Since *PlexA* constructs were expressed at different levels, we normalized each interaction between *Gyc76C* and *PlexA* to the corresponding *PlexA* expression level for that construct; this shows that the extracellular region of *PlexA* alone interacts with *Gyc76C* as strongly as FL *PlexA*, but suggests that the intracellular associations, though present, may be weaker (Fig. 2D; K.C. and A.L.K., unpublished). These experiments show that *Gyc76C* and *PlexA* can physically associate and suggest this association involves both extracellular and intracellular regions of these proteins.

Full-length Gyc76C exhibits guanylyl cyclase activity *in vitro*, and this activity is influenced by each Gyc76C protein domain

We generated a series of N-terminally Myc-tagged *Gyc76C* deletion constructs, each including one or two discrete protein domain deletions (Fig. 3A). Each of these *Gyc76C* constructs was expressed robustly in S2R+ cells (supplementary material Fig. S2A). Using a direct cGMP enzyme immunoassay (EIA) (Materials and methods), we measured total cGMP levels in S2R+ cells expressing wild-type Myc-FL *Gyc76C* or Myc-*Gyc76C*[D945A], in which a crucial amino acid (D945) in the guanylyl cyclase domain required for catalytic activity and semaphorin-mediated axon guidance in *Drosophila* (Thompson and Garbers, 1995; Ayoob et al., 2004) is mutated. We observed significant cGMP levels in S2R+ cells expressing Myc-FL *Gyc76C* but no detectable cGMP in cells expressing Myc-*Gyc76C*[D945A] (Fig. 3B), confirming *Drosophila* *Gyc76C* functions as a guanylyl cyclase.

Next, we assessed *Gyc76C* deletion constructs and found that each *Gyc76C* protein domain influences *Gyc76C*-mediated cGMP production *in vitro* (Fig. 3B). The Myc-*Gyc76C* construct that lacks the entire cytoplasmic domain (Δ Endo) did not produce cGMP levels above background (Fig. 3B). Deletion of the PDZ-binding motif (PBM) (Δ PBM, deleting the four C-terminal amino acids) completely abolished *Gyc76C* guanylyl cyclase (GC) activity. Deletion of the entire extracellular domain (Δ Ecto) resulted in elevated cGMP production compared with FL *Gyc76C*, and this was abolished when either the TM, or the PBM, was also deleted. Deletion of the KHD (Δ KHD) resulted in greatly elevated GC activity compared with FL *Gyc76C*, consistent with previous studies

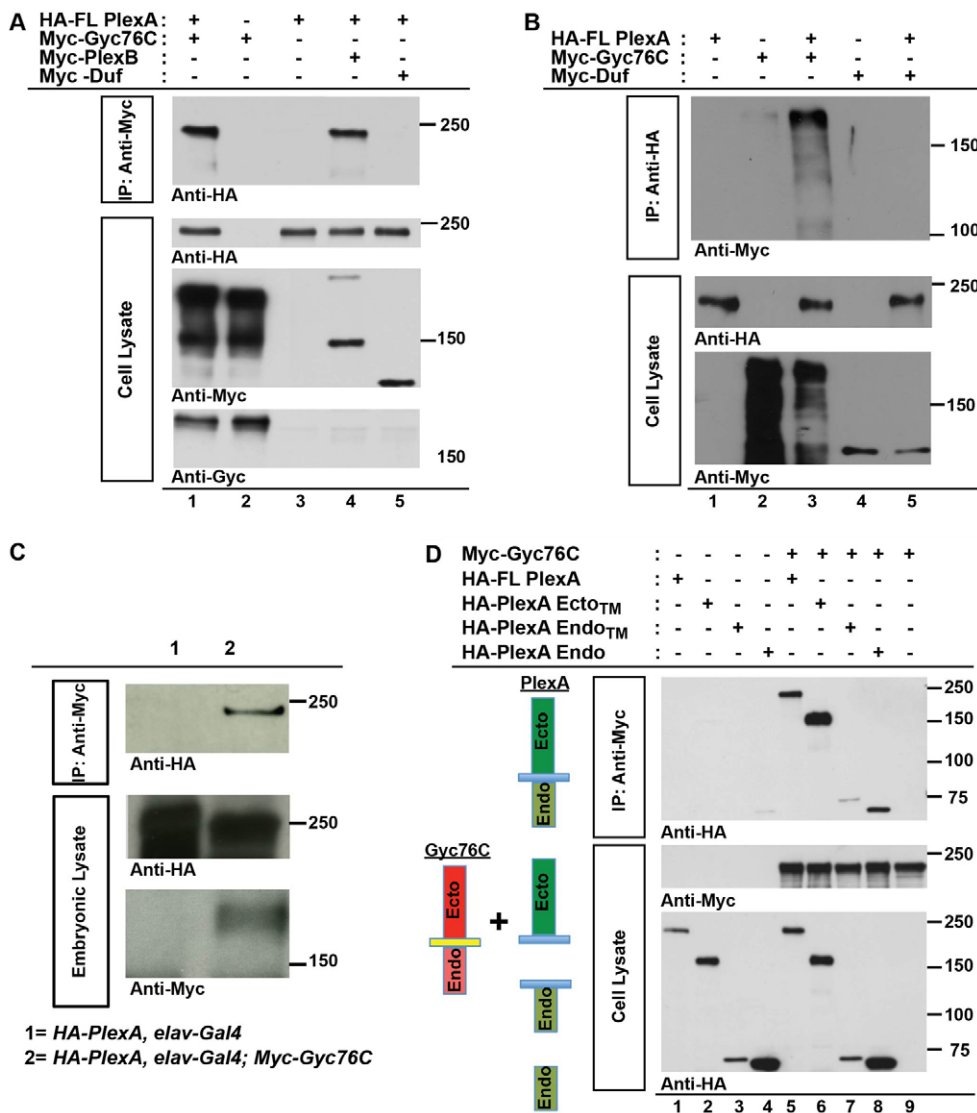


Fig. 2. Gyc76C physically associates with PlexA, both *in vitro* and *in vivo*.

(A,B) Lysates from *Drosophila* S2R+ cells expressing full-length (FL) Myc-Gyc76C with, or without, FL HA-PlexA were immunoprecipitated using anti-Myc and blotted with anti-HA to detect the presence of HA-PlexA (A, lane 1). IPs were also performed using anti-HA and blotted with anti-Myc to detect the presence of Myc-Gyc76C (B). FL Myc-PlexB immunoprecipitates FL HA-PlexA (lane 4, positive control), whereas Myc-Duf fails to immunoprecipitate FL HA-PlexA (lane 5, negative control). FL HA-PlexA immunoprecipitates FL Myc-Gyc76C (lane 3); however, FL PlexA fails to immunoprecipitate Myc-Duf (lane 5, negative control). 0.5% (3.75 μ l/lane) of total cell lysate (750 μ l) was loaded for the input; 20% (10 μ l/lane) of the total immunoprecipitate (50 μ l) was loaded for the IP. (C) Lysates from embryos expressing Myc-Gyc76C under the control of *elav-Gal4* with, or without, HA-PlexA were immunoprecipitated using anti-Myc and blotted with anti-HA to detect the presence of HA-PlexA (lane 2). 0.5% (2.5 μ l/lane) of total embryo lysate (500 μ l) was loaded for the input; 20% (10 μ l/lane) of the total immunoprecipitate (50 μ l) was loaded for the IP. (D) Lysates from S2R+ cells expressing FL Myc-Gyc76C with, or without, FL HA-PlexA (or several PlexA deletion constructs) were immunoprecipitated using anti-Myc and then blotted with anti-HA to detect the presence of HA-PlexA constructs. 0.5% (3.75 μ l/lane) of the total embryonic lysate (750 μ l) was loaded for the input; 25% (10.25 μ l/lane) of the total immunoprecipitate (50 μ l) was loaded for the IP.

demonstrating that the mammalian KHD negatively regulates cGMP production (Chinkers and Garbers, 1989; Potter, 2011). cGMP levels produced by Gyc76C lacking both KHD and PBM domains (Δ KHD+PBM) were greatly reduced compared with Δ KHD alone; however, these cGMP levels were significantly higher than FL Gyc76C. Deletion of the dimerization domain (Δ DD) abolished all GC, like vertebrate receptor GCs (Chinkers and Garbers, 1989). Finally, deletion of the unique Gyc76C C-terminal domain (Δ Cterm) yielded very low cGMP levels, and deletion of both Cterm and PBM abolished GC activity (Fig. 3B).

Protein expression levels and localization could contribute to differences in GC activity. We assessed total protein levels for all Gyc76C constructs using western blot analyses (supplementary material Fig. S2A), and also determined cell surface protein expression levels using live cell surface immunostaining (supplementary material Fig. S2B). Some of these modified Gyc76C proteins exhibited different total protein expression levels, and also some showed more robust cell surface localization than others. For example, both Δ Ecto and Δ KHD proteins are robustly localized to the cell surface (supplementary material Fig. S2B, top) and exhibit high GC activity (\sim 5–10 times FL Gyc76C). However, total protein expression levels produced by these constructs are comparable with,

or lower than, FL Gyc76C (supplementary material Fig. S2A, lanes 2, 4 and 7). Several constructs that show low-to-no GC activity do show robust cell surface localization (Gyc76C[D945A], Δ Cterm, Δ Cterm+PBM and Δ Endo; supplementary material Fig. S2B). Deletion of the PBM alone, or with the Ecto or KHD domain, does not significantly alter total protein expression levels compared with FL Gyc76C (supplementary material Fig. S2A, lanes 2, 5, 8, and 13); however, it does reduce cell surface protein localization (supplementary material Fig. S2B, middle). Nevertheless, Δ KHD+PBM shows robust GC activity (\sim 3 times FL Gyc76C). We observed low cell surface protein localization and total protein for the Δ DD construct (supplementary material Fig. S2B, middle). For Δ Ecto+TM, total protein levels are high; however, as expected, this variant shows no cell surface localization (supplementary material Fig. S2B, bottom). Biochemical assessments of cell-surface protein levels employing biotinylation of cell-surface proteins revealed protein levels for each Gyc76C deletion variant commensurate with cell-surface labeling experiments (K.C. and A.L.K., unpublished). Therefore, though there are differences in total protein expression and cell-surface localization of Gyc76C variants, except for Δ DD, these do not account for the differences in GC activity we observe among these Gyc76C proteins. Δ Cterm and Δ Cterm+PBM show robust total

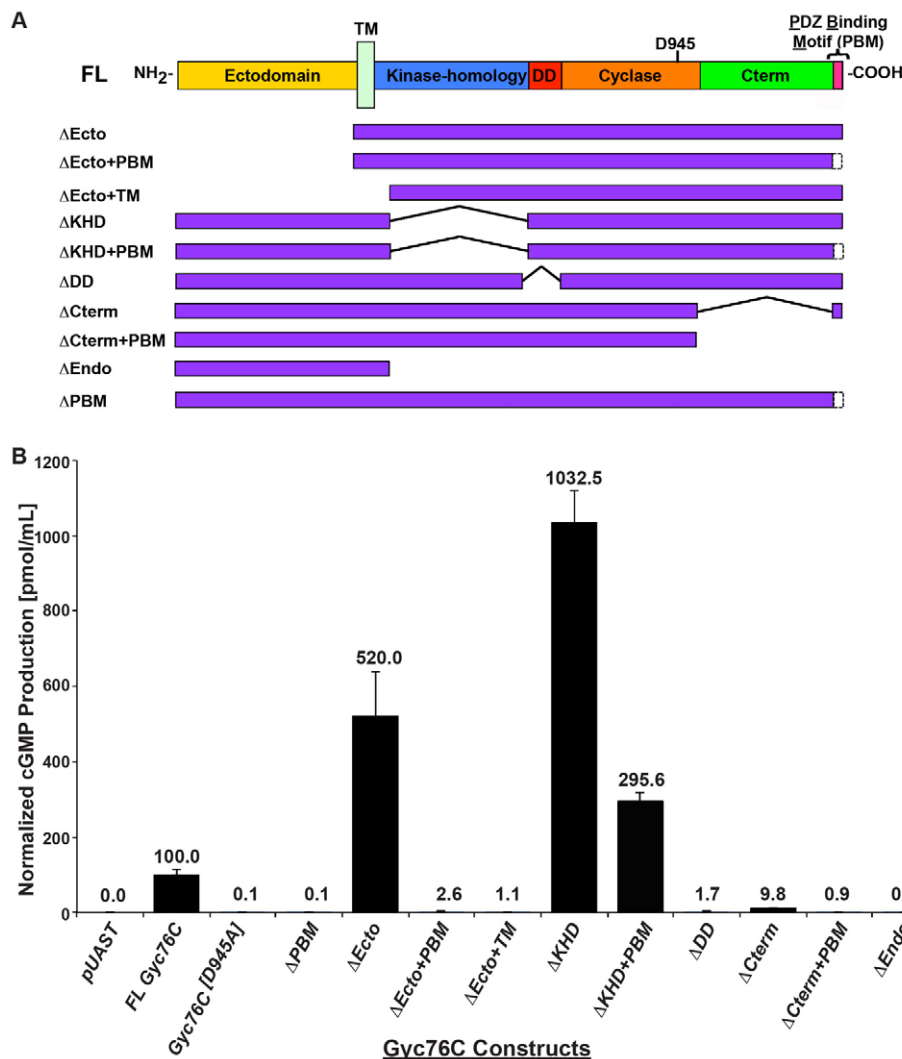


Fig. 3. Full-length Gyc76C exhibits guanylyl cyclase activity, and this activity is influenced by each Gyc76C protein domain. (A) Protein domain organization of FL Gyc76C and deletion constructs used in this study. D945 is the conserved aspartate residue required for guanylyl cyclase catalytic activity. (B) Normalized total cGMP levels in S2R+ cells expressing FL Gyc76C or Gyc76C deletion constructs (transfections performed in triplicate, cells were harvested 2 days after transfection). 5×Myc was tagged to the N terminus of each construct. cGMP levels were first measured in lysates derived from cells expressing each transgene and then normalized to the protein expression level of FL Gyc76C, as determined by western blot analysis (Materials and methods).

and cell-surface protein expression but produce no cGMP, suggesting that specific molecular mechanisms regulate Gyc76C cyclase activity. These experiments show that each Gyc76C protein domain influences cGMP production and suggest Gyc76C GC activity is regulated by both extracellular and intracellular mechanisms.

Gyc76C protein domain requirements for motor axon guidance rescue in *Gyc76C* mutant embryos

To investigate Gyc76C protein domain function *in vivo*, we generated 12 different *Gyc76C* transgenic fly lines (two independent fly lines per transgene), each expressing an altered Gyc76C lacking a different protein domain (ΔEcto, ΔKHD, ΔDD, ΔCterm, ΔEndo and ΔPBM). Each transgene included an N-terminal Myc, and we drove neuronal expression of these transgenes to determine the ability of each to rescue *Gyc76C* motor axon defects (Fig. 4A). Gyc76C protein expression levels in each transgenic line, assessed using quantitative western blot analysis, revealed that these constructs vary somewhat in their expression levels. However, each pair of independent transgenic lines harboring the same *Gyc76C* deletion construct showed comparable expression, and in all cases total protein levels were either equal to, or significantly greater than, those observed for FL Gyc76C (supplementary material Fig. S3A). Therefore, variations in expression of the deletion constructs are not due to positional effects on transgene expression. Similar to ISNb motor axon pathways, SNa axons also

display stereotypic neuromuscular connectivity; they navigate past the ventral longitudinal muscle field to innervate lateral transverse muscles 22, 23 and 24 (Landgraf et al., 1997), and together with the ISNb allow for assessment of motor axon guidance *in vivo* (Araújo and Tear, 2003). *Gyc76C* mutant embryos show significant defects in these motor axon pathways (Ayoob et al., 2004). These defects are not a secondary consequence of longitudinal muscle defects because overall muscle organization in *Gyc76C* mutant embryos is apparently normal (supplementary material Fig. S3B,B'). Furthermore, Gyc76C expression in somatic muscles fails to rescue motor axon guidance defects in *Gyc76C* homozygous mutants (K.C. and A.L.K., unpublished).

The only *Gyc76C* transgenic flies that rescue the ISNb and SNa defects observed in *Gyc76C*-null mutants are the two independent FL *Gyc76C* transgenes [FL(65) and FL(5.2)]. In these flies, ISNb and SNa pathway defects observed in *Gyc76C^{ext173}*-null mutants were rescued from 42% to 21%, and from 39% to 20%, respectively (Fig. 4A, red highlight; $P < 0.005$; comparable with previous experiments; Ayoob et al., 2004). All other *Gyc76C* deletion constructs failed to rescue ISNb or SNa defects (Fig. 4A). ΔDD, ΔCterm, ΔEndo and ΔPBM exhibit no GC activity in *in vitro* GC assays, and so elevated expression levels of proteins encoded by these constructs, compared with FL Gyc76C (supplementary material Fig. S3B, lanes 6–13), are not likely to result in elevated

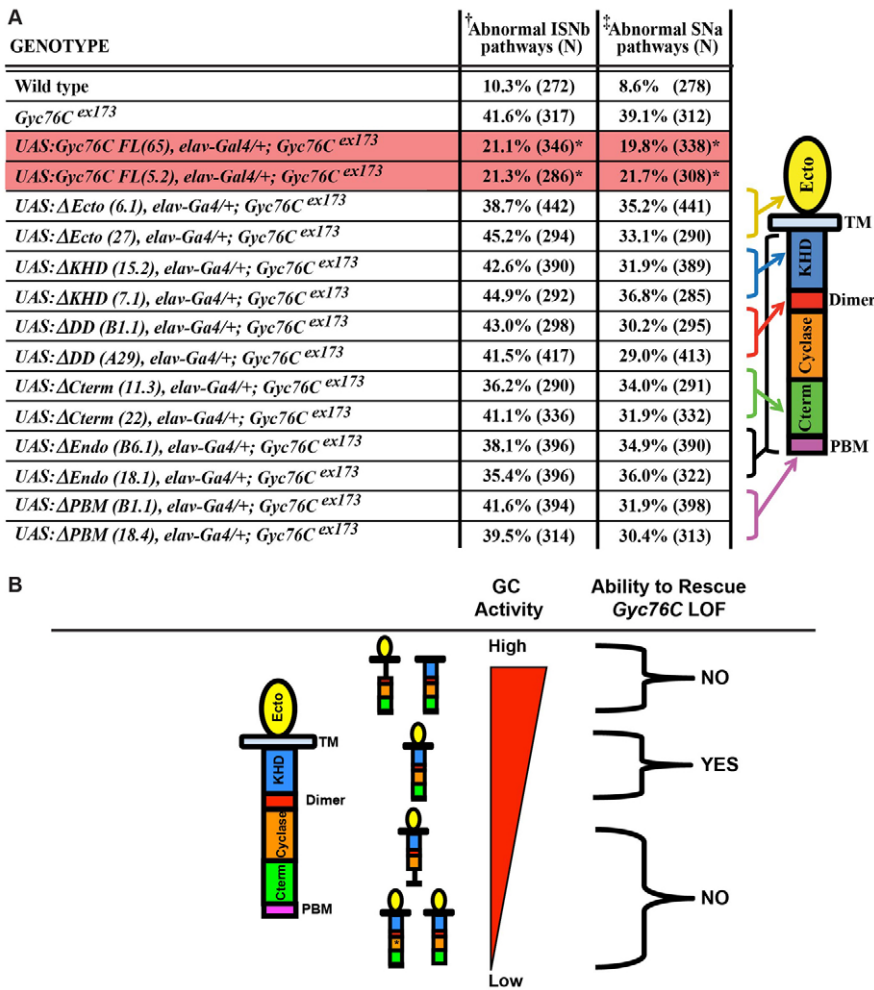


Fig. 4. *Gyc76C* protein domain requirements for rescue of motor axon guidance defects in the *Gyc76C* loss-of-function mutants. (A) Quantification of ISNb and SNa phenotypes in the *Gyc76C* loss-of-function mutant embryos and in rescue experiments using various *Gyc76C* deletion constructs. [†]ISNb phenotypes: failure of RP5 or RP3 ISNb axons to innervate ventral longitudinal muscles 12/13 or 6/7. [‡]SNa phenotypes: failure of SNa axons to defasciculate at choice points, to reach muscle 24 and/or to project along appropriate trajectories. *N*, number of hemisegments scored per genotype. *Significantly different from *Gyc76C^{ex173}* homozygous mutants. Z-test for two proportions; *P*<0.005. (B) The relationship between *in vitro* GC activity and *in vivo* rescue ability of FL *Gyc76C* and various domain deletions.

cGMP production. By contrast, ΔEcto and ΔKHD exhibit the highest *in vitro* GC activities, yet these two constructs do not rescue the motor axon defects in *Gyc76C* mutants; ISNb and SNa defects are phenotypically comparable, both quantitatively and qualitatively, with those observed in *Gyc76C*-null mutants (Ayoob et al., 2004), suggesting that motor axon pathfinding defects in unrescued embryos are not the result of dominant-negative effects from *Gyc76C* variants.

Taken together, these results suggest that *Gyc76C* cyclase activity is regulated by both extracellular and intracellular protein domains. The unique *Gyc76C* C terminus, and also the PBM, are crucial for normal cyclase activity *in vitro*, suggesting that signaling components exist that interact with *Gyc76C* and regulate its function.

PlexA augments cGMP levels produced by *Gyc76C* *in vitro*

We next investigated whether the PlexA receptor influences *Gyc76C* GC activity, employing the direct cGMP EIA assay described above and a different *Drosophila* cell line, DmBG2, to assess whether or not a functional relationship exists between *Gyc76C* and PlexA. Unlike S2R+ cells, which are derived from a macrophage-like lineage, DmBG2 cells are derived from the *Drosophila* third instar larval CNS (Yanagawa et al., 1998). A constant amount of the construct encoding FL *Gyc76C* DNA (or CD8-GFP as a control), 0.04 μg, was co-transfected into DmB2 cells with 0.2 μg (5×), 0.04 μg (1×) or 0.008 μg (1/5×) of the construct encoding FL PlexA DNA. The amount of PlexA DNA transfected into DmBG2 cells in

these experiments directly correlates with PlexA protein levels (supplementary material Fig. S4, top panel). When fivefold more PlexA DNA compared with *Gyc76C* DNA was transfected into DmBG2 cells, total cGMP levels were increased by ~2.4-fold over what we observed for *Gyc76C* alone (Fig. 5A, representative experiment; Fig. 5B, average fold change, four independent experiments). In the absence of transfected FL *Gyc76C*, FL PlexA alone had no significant effect on cGMP levels in DmBG2 cells. Different amounts of PlexA DNA transfected into DmBG2 cells in these experiments did not affect *Gyc76C* protein expression levels (supplementary material Fig. S4, bottom panel, lanes 1-4). We performed similar GC assays with ΔEcto, ΔKHD or ΔPBM; however, 5×PlexA did not increase GC activity of these constructs (K.C. and A.L.K., unpublished). PlexA-mediated augmentation of *Gyc76C* GC activity is consistent with our genetic analyses showing that *Gyc76C* influences *Sema-1a* gain-of-function phenotypes in the PNS (this study), and also *PlexA*-dependent gain-of-function phenotypes in the CNS (Ayoob et al., 2004), supporting a model whereby *Gyc76C* facilitates *Sema-1a*/PlexA-mediated axon repulsion.

A PDZ domain-containing protein, dGIPC, interacts with *Gyc76C* and increases cell surface expression of *Gyc76C* *in vitro*

Our *in vitro* and *in vivo* results suggest that there may be PDZ (PSD95/Dlg1/ZO-1) domain-containing proteins that interact with

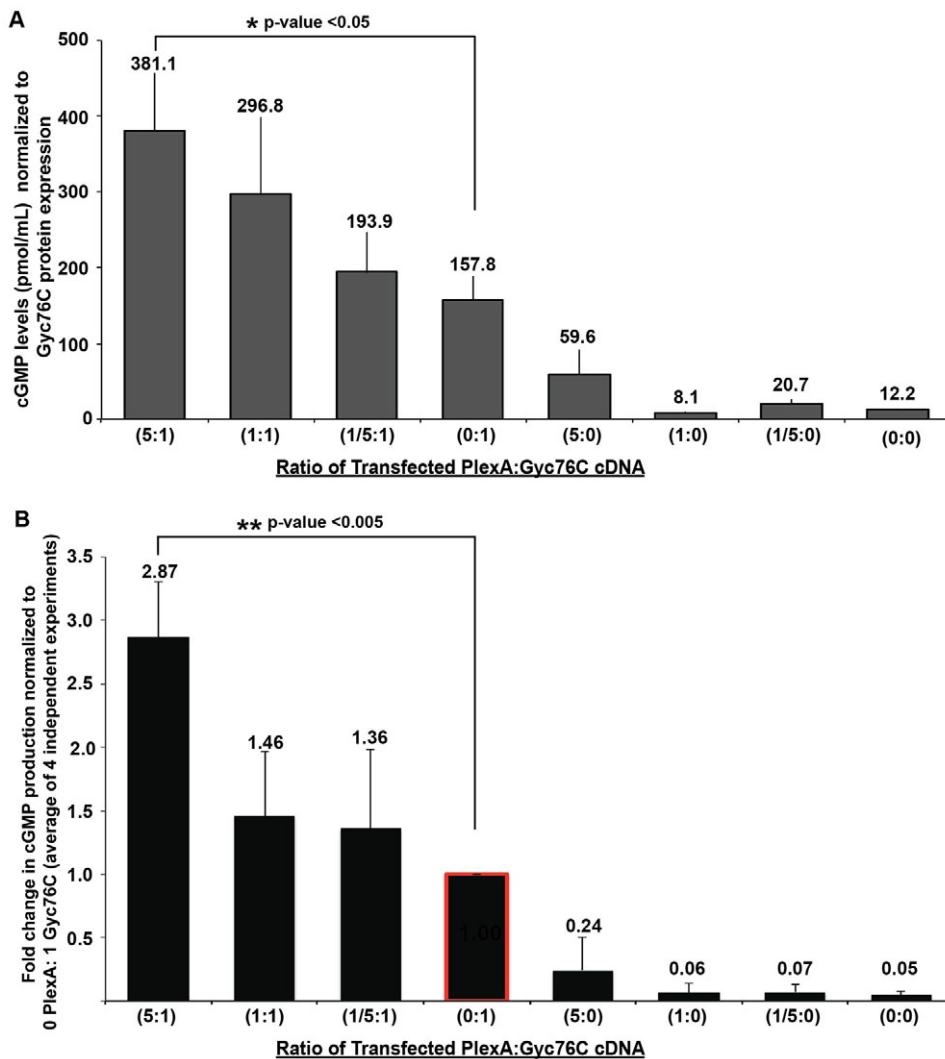


Fig. 5. PlexA augments Gyc76C cGMP production *in vitro*. (A) Quantification of a single experiment showing normalized cGMP production resulting from transfection with FL Gyc76C and varying levels of FL PlexA in DmBG2 cells grown for 3.5 days in culture. 0.2 μ g (5 \times), 0.04 μ g (1 \times) or 0.008 μ g (1/5 \times) of FL PlexA cDNA was transfected with a constant amount (0.04 μ g) of FL Gyc76C (or CD8-GFP as a control). Average cGMP levels were determined from cell lysates (transfections performed in triplicate) and normalized to Myc-FL Gyc76C expression (see Materials and methods). Error bars indicate s.d. of cGMP levels in triplicate samples from this representative GC assay. *Significantly different from cGMP levels measured in 1 \times FL Gyc76C alone (*t*-test for two proportions; $P < 0.05$). (B) Fold change in normalized cGMP production determined from four independent GC assays, as described in A. Error bars indicate s.d. for each condition for cGMP production determined from four independent GC assays. **Significantly different from 1 \times FL Gyc76C alone (*t*-test for two proportions; $P < 0.005$).

Gyc76C and regulate its function. We used the C-terminal 75 amino acids of Gyc76C, which include the PDZ-binding motif, as a bait (KC1) to search for Gyc76C-interacting proteins, screening a *Drosophila* embryonic (0–24 hours) yeast two-hybrid (Y2H) cDNA library (supplementary material Fig. S5A; Materials and methods). Clones encoding interacting proteins were further examined using another bait (KC2) that is similar to KC1 but lacks the PDZ-binding motif (supplementary material Fig. S5A). We found that clones that interacted with KC1 but not KC2 encoded the *Drosophila* GAIP interacting protein, C terminus homolog (dGIPC; Kermit – FlyBase) (Djiane and Mlodzik, 2010).

There are three mammalian, two *Xenopus* and one *Drosophila* GIPC. GIPC is an intracellular protein with a centrally located PDZ domain and no other conserved sequence motifs. GIPC interacts with RGS-GAIP (regulator of G protein signaling-GTPase activating protein for Gai) (De Vries et al., 1998) and also with other GIPC-binding partners (Cai and Reed, 1999; Wang et al., 1999; Lou et al., 2001; Tan et al., 2001). GIPC is implicated in regulating the distribution of the Sema-5A protein (Wang et al., 1999) and NMDA receptor trafficking (Yi et al., 2007) *in vitro*. The *Drosophila* GIPC homolog, dGIPC, was first described in a gain-of-function screen designed to identify planar cell polarity genes in *Drosophila* (Djiane and Mlodzik, 2010). dGIPC is also important for locomotor activity

and longevity, possibly through the regulation of dopamine (DA) receptor trafficking (Kim et al., 2010).

We performed *in vitro* co-IP experiments, expressing HA-dGIPC with Myc-FL Gyc76C, Myc- Δ PBM, Myc- Δ Cterm, Myc- Δ Cterm+PBM, Myc- Δ Endo or GFP in S2R+ cells. Immunoprecipitation of HA-dGIPC with anti-HA revealed a robust interaction between Gyc76C and dGIPC. This was greatly attenuated when the Gyc76C PBM domain was removed (Fig. 6A, lanes 1 and 2, asterisk), and was completely abolished when the Gyc76C C-terminal region, the Gyc76C C-terminal region plus the PBM or the entire intracellular region of Gyc76C was deleted (Fig. 6A, lanes 3–5). These experiments demonstrate that dGIPC interacts with Gyc76C *in vitro*, requiring the PBM domain and, to a much lesser extent, other Gyc76C C-terminal sequences.

Since mammalian GIPC regulates the distribution of several transmembrane proteins (Wang et al., 1999; Tan et al., 2001; Yi et al., 2007), we asked whether dGIPC influences cell surface localization of Gyc76C. Using biotinylation cell surface protein labeling assays, we found a significant increase in the levels of Gyc76C protein localized to the plasma membrane of S2R+ cells overexpressing dGIPC (Fig. 6B, lanes 2 and 4). This result suggests that dGIPC regulates Gyc76C GC activity by influencing Gyc76C cell surface distribution.

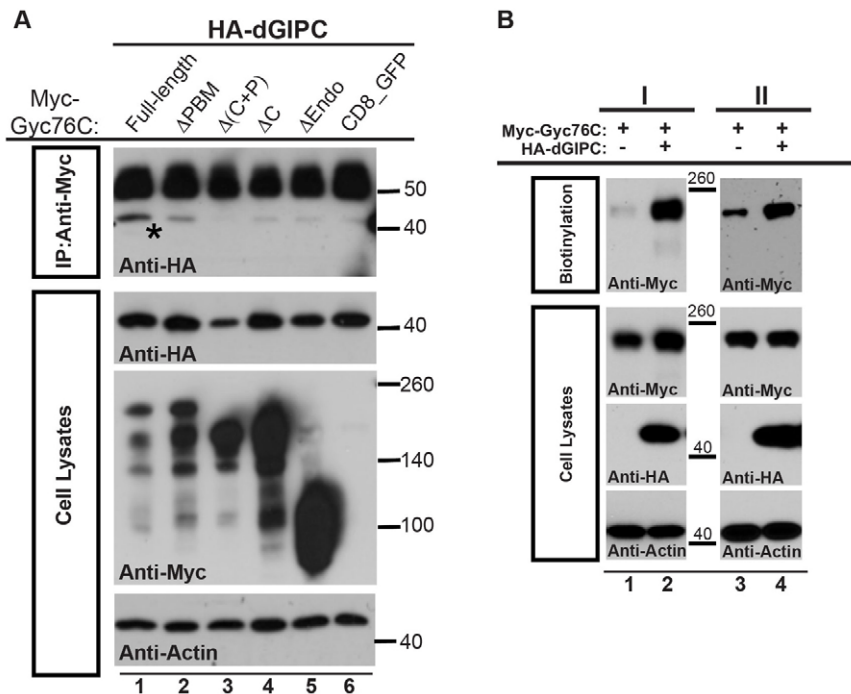


Fig. 6. dGIPC physically interacts with Gyc76C and increases Gyc76C cell surface localization *in vitro*.

(A) CoIP of S2R+ cell lysates expressing HA-dGIPC with, or without, FL Myc-Gyc76C. (B) Biotinylation of S2R+ cells expressing FL Myc-Gyc76C and HA-dGIPC prior to cell lysis. Two independent experiments (I, II) show a significant increase of biotinylated Gyc76C with dGIPC (compare lanes 1 and 3 with lanes 2 and 4).

dGIPC is required for embryonic motor axon guidance and genetically interacts with *Gyc76C*, *Sema1a* and *PlexA*

We next examined dGIPC function in motor axon guidance and observed significant defects in the ISNb (46.1%) and SNa (31.5%) motor axon pathways in embryos trans-heterozygous for two chromosomal deficiency lines (*Df7890* and *Df8941*) that remove nine genes, including *dGIPC* (K.C. and A.L.K., unpublished). The *dGIPC^{ex31}* allele does not express dGIPC protein (Djiane and Mlodzik, 2010), and *dGIPC^{ex31}* homozygous embryos show pathfinding defects in ISNb (35.5%) and SNa (30.4%) pathways; *dGIPC^{ex31}/Df8941* embryos exhibit 46.2% and 20.8% pathfinding defects in ISNb and SNa pathways, respectively. These phenotypes are qualitatively and quantitatively similar to those observed in *dGIPC^{ex31}* homozygous embryos. Furthermore, the predominant pathfinding defects are qualitatively similar to those we observed in *Gyc76C* homozygous mutant embryos, though the penetrance of SNa defects is somewhat lower. Together, these results show that the *dGIPC^{ex31}* allele is likely a null, or strong hypomorphic, allele of *dGIPC*.

Embryos heterozygous for *dGIPC* and either *Gyc76C*, *Sema1a* or *PlexA*, were assessed for trans-heterozygous genetic interactions to determine whether or not these genes function in the same genetic pathway (Artavanis-Tsakonas et al., 1995; Winberg et al., 1998b). *dGIPC^{ex31/+}; Gyc76C^{ex173/+}* embryos show 48.5% and 23.1% defects in ISNb and SNa pathways, respectively (Fig. 7A). *dGIPC* also genetically interacts with *Sema1a* and *PlexA*, as observed in *dGIPC^{ex31/+}; Sema1a^{P1/+}* and *dGIPC^{ex31/+}; PlexA^{Df(4)3C/+}* embryos (Fig. 7A). In these embryos, ISNb axons often fail to innervate their muscle targets with a penetrance comparable to that observed in *dGIPC^{ex31}* homozygotes.

Qualitatively and quantitatively these trans-heterozygous mutant embryos display ISNb phenotypes similar to *dGIPC* or *Gyc76C* homozygous mutant embryos, including stalling defects at M12/13 and at M6/7 (Fig. 7A). However, in these embryos we observe only mild SNa defects (Fig. 7A), suggesting that alterations in signaling in these trans-heterozygous embryos are not strong enough to affect

all motor axon pathways. We also analyzed motor axon pathways in *dGIPC^{ex31}; Gyc76C^{ex173}* double null mutants and observed that the penetrance of ISNb defects is similar to that observed in *dGIPC^{ex31}* or *Gyc76C^{ex173}* homozygous single mutants, whereas the penetrance of SNa defects is similar to *dGIPC^{ex31}* homozygous mutants (Fig. 7A, red box). These data suggest that *dGIPC* and *Gyc76C* function in the same genetic pathway, and together our genetic analyses support dGIPC functioning with *Gyc76C* in *Sema1a*/*PlexA*-mediated repulsion.

Neuronal dGIPC is required for embryonic motor axon pathfinding

dGIPC exhibits strong expression in CNS midline glia of the *Drosophila* ventral nerve cord (VNC) (Djiane and Mlodzik, 2010). *In situ* hybridization (ISH) with a *dGIPC*-specific cRNA antisense probe, and immunohistochemistry (IHC) using an antibody directed against dGIPC, revealed enriched dGIPC in the midline region of VNC wild-type embryos. This midline staining was absent when a *dGIPC* sense probe was used in ISH (K.C. and A.L.K., unpublished), or when *dGIPC^{ex31}*-null embryos were used in IHC experiments (Djiane and Mlodzik, 2010). However, we also detected weak, but significant, dGIPC protein expression in ventral nerve roots exiting the VNC (supplementary material Fig. S5B, red arrowheads) that is not present in *dGIPC*-null mutants (supplementary material Fig. S5B'). *dGIPC*-null mutants display motor axon defects, and so dGIPC could function in neurons, non-neuronal cells, or both. In the *Drosophila* brain, dGIPC is predominantly expressed in glial cells but is also expressed in DA neurons, and DA neuronal expression of dGIPC is crucial for locomotor activity (Kim et al., 2010).

To determine dGIPC cell type requirements, we employed *Gal4* drivers for *in vivo* rescue experiments *dGIPC^{ex31}* homozygous mutant embryos. We expressed *dGIPC* in all neurons using *elav-Gal4* in *dGIPC^{ex31}*-null mutant embryos and found significant rescue of both ISNb and SNa motor axon guidance defects (Fig. 7B,B'): from 35.5% to 17.7% and from 30.4% to 15.1%,

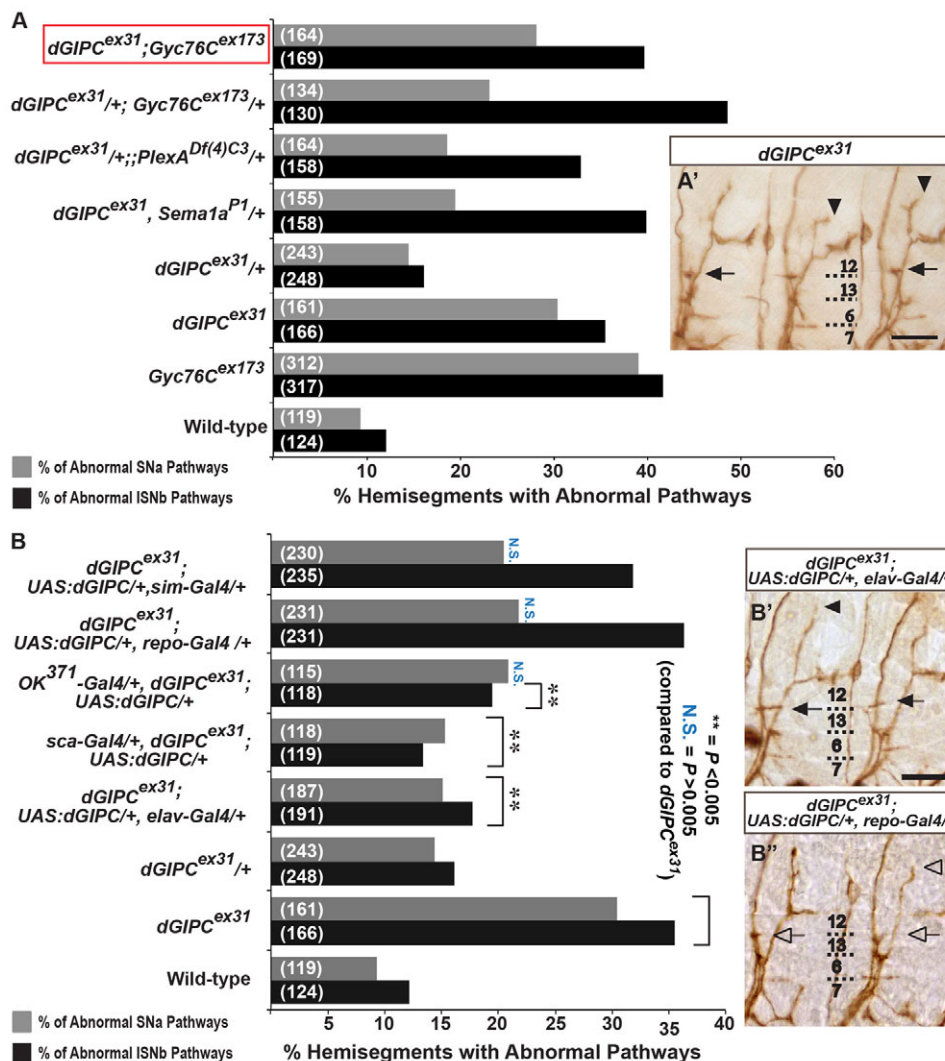


Fig. 7. *dGIPC* genetically interacts with *Gyc76C*, *Sema-1a* and *PlexA*, and is required in neurons for motor axon pathfinding. (A) Quantification of motor axon defects in *dGIPC* homozygous mutant embryos and genetic interactions between *dGIPC* and *Gyc76C*, *Sema-1a* or *PlexA*. Motor axon defects in *dGIPC*; *Gyc76C* homozygous double mutants are highlighted (red box). Numbers in parentheses, total number of hemisegments scored for ISNb or SNa pathways. (A') Filleted late stage 16 embryo stained with 1D4 revealing motor axons in abdominal segments. In a *dGIPC^{ex31}* homozygous mutant embryo, axons within the ISNb (black arrows) and SNa (black arrowheads) pathways often fail to reach their proper targets. Scale bar: 5 μ m. (B) Quantification of rescue experiments using *dGIPC* driven by cell type-specific *Gal4* drivers. **Significantly different from *dGIPC^{ex31}* homozygous mutants. Z-test for two proportions; $P < 0.005$. N.S., not significantly different from values for *dGIPC^{ex31}* homozygous mutants. (B', B'') Filleted late stage 16 embryos stained with 1D4 revealing motor axons in abdominal segments. (B') Neuronal *dGIPC* in a *dGIPC^{ex31}* mutant restores proper ISNb (black arrows) and SNa (black arrowhead) muscle innervation. (B'') Glial expression of *dGIPC* does not rescue ISNb (open arrows) or SNa muscle innervation (open arrowhead). Scale bar: 5 μ m. Anterior is leftwards; dorsal is upwards.

respectively (Fig. 7B). When *dGIPC* was expressed in all glial cells using the *repo-Gal4* (Sepp et al., 2001) driver, or in midline glial cells and MP1 CNS neurons using the *single-minded GAL4* (*sim-GAL4*) driver (Hidalgo and Brand, 1997), no rescue of ISNb defects (36.3% for *repo-Gal4*; 31.9% for *sim-Gal4*), and seemingly apparent but not statistically significant rescue of SNa defects (21.8% for *repo-Gal4*; 20.5% for *sim-Gal4*), were observed in *dGIPC^{ex31}*-null mutant embryos carrying *repo-Gal4* or *sim-Gal4* (Fig. 7B, B''). As *elav-Gal4* also drives expression in neural progenitors and embryonic glia (Berger et al., 2007), we employed two additional neuron-specific drivers: *scabrous-GAL4* (*sca-Gal4*) (Mlodzik et al., 1990) and *OK³⁷¹-Gal4* (Mahr and Aberle, 2006). Neuronal expression of *dGIPC* driven by *sca-Gal4* also rescues both ISNb (13.4%) and SNa (15.3%) motor axon defects in *dGIPC^{ex31}* homozygous mutant embryos (Fig. 7B). In *OK³⁷¹-Gal4/+*, *dGIPC^{ex31}*; *UAS:dGIPC/+* embryos, we observe significant rescue of the ISNb pathway (19.5%; $P < 0.005$), and seemingly apparent but not statistically significant rescue of the SNa pathway (20.9%; $P > 0.005$). Therefore, it remains uncertain whether *dGIPC* expression in glia or neurons rescues SNa defects in *dGIPC* mutants. However, neuronal *dGIPC* expression is required for proper ISNb pathfinding. These results show that *dGIPC* robustly associates with the PBM domain of *Gyc76C*, that

it is required for embryonic motor axon pathfinding, and that *dGIPC* strongly interacts with *Gyc7C*, *Sema-1a* and *PlexA*.

DISCUSSION

We provide here support for the *Drosophila* receptor guanylyl cyclase *Gyc76C* being a component of the *Sema1a*-*PlexA* signaling cascade *in vivo*. Each discrete *Gyc76C* protein domain is essential for *Gyc76C* catalytic activity *in vitro* and for motor axon guidance *in vivo*. Furthermore, the cytosolic protein *dGIPC* interacts with *Gyc76C* and functions in *Gyc76C*-mediated motor axon guidance. These results provide an *in vivo* link between semaphorin-mediated repulsive guidance and alteration of intracellular cGMP levels.

Gyc76C is part of the *Sema-1a*-*PlexA* signaling complex

The *Gyc76C*-*Sema-1a* gain-of-function genetic interactions we observe here are consistent with previous observations showing that *Gyc76C* loss and gain of function modifies aberrant CNS midline crossing by FasII⁺ longitudinal axons in a *PlexA* gain-of-function genetic background (Ayoob et al., 2004). Furthermore, we observe robust physical interactions between *Gyc76C* and *PlexA* both *in vitro* and *in vivo*, raising the possibility that *PlexA* regulates *Gyc76C*-mediated signaling. Co-expressing *PlexA* at high levels *in vitro* augments cGMP levels produced by *Gyc76C*. Future work will

establish whether extracellular, intracellular, or both, types of protein-protein associations between Gyc76C and PlexA are essential for regulating Gyc76C enzymatic activity.

Each Gyc76C domain is required for cyclase activity and proper motor axon guidance

Our Gyc76C structure-function analyses are consistent with the idea that PlexA binds to the extracellular and intracellular regions of Gyc76C to relieve inhibitory effects on GC activity from of Gyc76C intramolecular interactions, increasing cGMP levels within extending motor axon growth cones and affecting growth cone guidance. This is reminiscent of Sema-3A bath application increasing intracellular cGMP levels in *Xenopus* spinal neurons *in vitro* (Togashi et al., 2008), and our results suggest that intracellular cGMP produced by Gyc76C is required for Sema-1a-mediated repulsion. However, it is possible that signaling by intracellular cGMP is coupled with intracellular cAMP in Sema-1a-mediated repulsive guidance events (Nishiyama et al., 2003), and future work will determine whether varying the cAMP-to-cGMP ratio modulates Sema-1a-mediated repulsion, or converts it to attraction. Bath application of Sema-1a did not affect Gyc76C-PlexA physical associations or Gyc76C-PlexA-mediated cGMP production (K.C. and A.L.K., unpublished), suggesting that Sema-1a-dependent regulation of intracellular cGMP levels could involve ligand-gated, dynamic, spatiotemporal regulation of GC activity; visualizing this signaling event will require real-time imaging of cGMP during repulsive growth cone steering.

The small GTPase Rac and its downstream effector p21 activated kinase (PAK) can regulate receptor GCs to raise cellular cGMP levels in fibroblasts *in vitro*, and the kinase domain of PAK interacts with the cyclase domain of receptor GC-E (Guo et al., 2007; Guo et al., 2010); PAK, therefore, may associate with Gyc76C and regulate this receptor GC during axon pathfinding.

dGIPC interacts with Gyc76C and is required for motor axon guidance in *Drosophila*

The deletion of the Gyc76C PBM strongly suppresses cGMP production by FL Gyc76C, and Gyc76C variants lacking the PBM motif exhibit low cell-surface expression levels, suggesting dGIPC regulates Gyc76C cell-surface localization. PDZ-containing proteins could form a protein scaffold required for plasma membrane localization of the Sema-1a-PlexA/Gyc76C signaling complex, and we find that the PDZ domain-containing dGIPC protein interacts with Gyc76C. In vertebrates, GIPC regulates protein trafficking, subcellular localization and various signaling events (De Vries et al., 1998; Cai and Reed, 1999; Wang et al., 1999; Lou et al., 2001; Tan et al., 2001; Yi et al., 2007). Gyc76C cell-surface localization is enhanced *in vitro* in the presence of dGIPC, and this may serve to regulate Gyc76C-mediated signaling. dGIPC genetic analyses show that dGIPC plays a neuronal role in motor axon guidance, and this likely occurs through interactions that modulate Gyc76C-mediated cGMP signaling. Mammalian GIPC forms dimers and multimeric complexes (Bunn et al., 1999; Gao et al., 2000; Hirakawa et al., 2003; Jeanneteau et al., 2004; Kedlaya et al., 2006; Naccache et al., 2006; Varsano et al., 2006). dGIPC may be a part of a molecular scaffold that couples Gyc76C to cell membrane trafficking machinery or anchors Gyc76C to the plasma membrane. Alternatively, dGIPC may be essential for activating or transducing Gyc76C-mediated cGMP signaling in axon guidance events. Future genetic and biochemical analyses will reveal the downstream signaling components that respond to changes in cGMP levels *in vivo* and direct discrete neuronal growth cone steering responses.

MATERIALS AND METHODS

Drosophila strains and phenotypic characterization

Culturing *Drosophila* was performed as described previously (Yu et al., 1998; Terman et al., 2002; Ayoob et al., 2004). Stocks *Df7860* and *Df8941* were from the Bloomington Stock Center. Gal4 drivers were: *elav(2)-GAL4*, *elav(3E)-GAL4* (Yao and White, 1994), *Mef2-Gal4* (Ranganayakulu et al., 1996), *sim-Gal4* (Hülsmeier et al., 2007), *repo-Gal4* (Sepp et al., 2001), *OK³⁷¹-Gal4* (Ramadan et al., 2007) and *Sca-GAL4* (Klaes et al., 1994). Analyses of axon guidance defects performed as described previously (Yu et al., 1998).

Gyc76C deletion constructs

Gyc76C (amino acids 1-1525) domains are defined as Ecto (1-492), TM (494-514), KHD (517-812), DD (815-870), Cterm (1105-1521), Endo (517-1525) and PBM (1522-1525). PlexA (amino acids 1-1945) domains are defined as: Ecto_{TM} (1-1330), TM (1282-1300), Endo_{TM} (1271-1945) and Endo (1305-1945). Endogenous Gyc76C or PlexA signal peptide replaced with Igk-leader sequence, followed by 5×Myc (EQLISEEDL) or 2×HA (YPYDVPDYA), respectively. dGIPC from a cDNA clone was C-terminally tagged with 2×HA. Constructs were inserted into pUAST (Brand and Perrimon, 1993); UAS-CD8-EGFP (pUAST-DEST16) obtained from the *Drosophila* Genomics Resource Center.

Cell culture

S2R+ cells were grown in Schneider's medium (Invitrogen) with 10% heat-inactivated fetal bovine serum (FBS); ML-DmBG2 cells were grown in Shields and Sang M3 medium with 10% heat-inactivated FBS and 10 µg/ml insulin. Both cells types were cultured at 25°C [procedures can be found at DRSC (<http://www.flyrnai.org/DRSC-PRC.html>)].

Co-immunoprecipitation assays

Drosophila S2R+ cells were transfected with pUAST:5×Myc-FL Gyc76C with, or without, full-length pUAST:2×HA-FL PlexA using Effectene (Qiagen). Forty-eight hours later, cell lysates were immunoprecipitated with anti-Myc monoclonal antibody (9E10; Sigma) and blotted with anti-HA monoclonal antibody at 1:2500 (12CA5; Roche); alternatively, cell lysates were immunoprecipitated using anti-HA (12CA5) and immunoblotted using anti-Myc (9E10) at 1:2500. For *in vivo* co-immunoprecipitation, *UAS:HA-PlexA*, *elav-Gal4/Cyo* flies were crossed to either *UAS:Myc-FL Gyc76C* or wild-type flies. Embryonic lysates were isolated and immunoprecipitated with anti-Myc (9E10) (Terman et al., 2002). Immunoprecipitates were probed using anti-HA (12CA5) at 1:2500 and anti-Myc (9E10) at 1:2500.

Guanylyl cyclase activity assay

In vitro cGMP concentrations determined from cell lysates with the Direct cGMP Enzyme Immunoassay Kit (Assay Designs, # 900-014). S2R+ cells and ML-DmBG2 cells were transfected for 36 hours or 72 hours, respectively. Each well of a 24-well plate was plated with 0.5×10^6 cells. Transfected cells were incubated with 0.5 mM IBMX in serum-free medium for 30 minutes at room temperature with gentle rocking, washed once with 1×PBS, lysed in 0.1 M HCl for 15 minutes at room temperature, and spun at 600 g for 5 minutes. Supernatants were diluted four- or fivefold in 0.1 M HCl for cGMP concentration determination. Expression of FL Gyc76C and the Gyc76C construct variants in western blots were quantified using ImageJ and normalized using actin controls. Raw cGMP levels produced by each Gyc76C variant were then normalized to the protein expression level of FL-Gy76C (raw cGMP levels × [(FL-Gy76C protein expression/corresponding actin loading control)/(individual construct protein expression/corresponding actin loading control)]).

Immunohistochemical analyses

Embryo collections and staining were performed as described (Yu et al., 1998; Ayoob et al., 2004). Primary antibodies used were: anti-FasII mAb 1D4 (1:4; Van Vactor et al., 1993), rabbit anti-Sema-1a (1:500; Yu et al., 1998), mouse anti-MHC (1:1000; Sigma), mouse anti-dGIPC (1:250; Djiane and Mlodzik, 2010), anti-Myc 9E10 (1:500; Sigma) and anti-HA 12CA5 (1:500; Roche). HRP-conjugated goat anti-mouse and anti-mouse IgG/M

(1:500; Jackson ImmunoResearch), and Alexa488-conjugated goat anti-mouse IgG, Alex546-conjugated goat anti-rabbit IgG and Alex647-conjugated goat anti-rabbit IgG (all 1:500; Molecular Probes) were the secondary antibodies.

Live cell-surface immunostaining and biotinylation

S2R+ cells were transfected with Gyc76C constructs for 2 days. For live cell surface immunostaining, transfected cells were blocked in ice-cold 10% FBS/S2 medium on ice for 10 minutes, incubated with anti-Myc 9E10 (1:100)/10%FBS/S2 medium on ice for 30 minutes and washed with ice-cold 3% sucrose/PBS. Cells were fixed in 4% paraformaldehyde/3% sucrose for 10 minutes, permeabilized with 0.5% triton/PBS for 5 minutes, blocked in 10% NGS/PBS for 15 minutes and incubated with rabbit anti-Myc 71D10 (1:500; Cell Signaling) overnight at 4°C. Secondary antibodies were Alexa 488-conjugated goat anti-mouse IgG (1:500) and Alexa647-conjugated goat anti-rabbit IgG (1:500; Molecular Probes). In biotinylation cell surface protein assays, transfected cells were washed twice with ice-cold PBS, incubated with 1 mg/ml EZ-link Sulfo-NHS-SS-Biotin (Thermo Scientific) on ice for 20 minutes, washed twice with ice-cold PBS and then incubated with 50 mM glycine on ice for 10 minutes prior to lysis in RIPA buffer and sonication. Homogenates were centrifuged at 23,000 *g* for 20 minutes at 4°C, supernatants were incubated with NeutrAvidin beads (Thermo Scientific) for 2 hours at 4°C and washed four times with Wash buffer [150 mM NaCl, 50 mM Tris (pH 8.0), 1 mM MgCl and 1% NP40]. Precipitates were analyzed by western blot using anti-Myc 9E10 (1:2000).

Yeast two-hybrid screen

Yeast protocols used standard techniques (Golemis et al., 1994; Terman et al., 2002). The Gyc76C intracellular domain (amino acids 1451-1525) was PCR amplified and inserted into yeast expression vector pEG202 (bait vector) to generate KC1 bait. KC1 was introduced into yeast strain EGY48, containing the β -galactosidase-expressing plasmid pJK103. Western analysis of transformed yeast using anti-LexA (Invitrogen) confirmed expression of appropriately sized bait protein (unpublished data), and an activation assay showed that the bait did not activate transcription (K.C. and A.L.K., unpublished). A 0-24 hour *Drosophila* embryonic cDNA library was cloned into the yeast expression vector pJG4-5. Greater than 2×10^6 clones were screened and interactions assessed using a visual β -galactosidase assay and a test of growth in the absence of leucine. Interacting yeast clones were selected, and standard protocols were used to recover the library vector and sequence clones on both strands. Over 30 interactors were identified and subjected to secondary screen using a different bait, KC2, lacking the PDZ-binding motif (amino acids 1434-1521).

Acknowledgements

We thank Drs Djiane and Mlodzik for generously providing dGIPC antibody and dGIPC mutant flies, DGRC and Bloomington Stock Centers for fly stocks, and Afshan Ismat for assistance with ISH experiments. We thank S. Jeong and X. Xie for critical reading of the manuscript.

Competing interests

The authors declare no competing financial interests.

Author contributions

K.C. and A.L.K. designed experiments; K.C. performed experiments; K.C. and A.L.K. analyzed data and wrote the manuscript.

Funding

This work was supported by The National Institutes of Health [NS35165] to A.L.K. A.L.K. is an Investigator of the Howard Hughes Medical Institute. Deposited in PMC for release after 6 months.

Supplementary material

Supplementary material available online at <http://dev.biologists.org/lookup/suppl/doi:10.1242/dev.095968/-/DC1>

References

- Araújo, S. J. and Tear, G. (2003). Axon guidance mechanisms and molecules: lessons from invertebrates. *Nat. Rev. Neurosci.* **4**, 910-922.
- Artavanis-Tsakonas, S., Matsuno, K. and Fortini, M. E. (1995). Notch signaling. *Science* **268**, 225-232.

- Ayoob, J. C., Yu, H. H., Terman, J. R. and Kolodkin, A. L. (2004). The *Drosophila* receptor guanylyl cyclase Gyc76C is required for semaphorin-1a-plexin A-mediated axonal repulsion. *J. Neurosci.* **24**, 6639-6649.
- Bashaw, G. J. and Klein, R. (2010). Signaling from axon guidance receptors. *Cold Spring Harb. Perspect. Biol.* **2**, a001941.
- Berger, C., Renner, S., Lüer, K. and Technau, G. M. (2007). The commonly used marker ELAV is transiently expressed in neuroblasts and glial cells in the *Drosophila* embryonic CNS. *Dev. Dyn.* **236**, 3562-3568.
- Brand, A. H. and Perrimon, N. (1993). Targeted gene expression as a means of altering cell fates and generating dominant phenotypes. *Development* **118**, 401-415.
- Bunn, R. C., Jensen, M. A. and Reed, B. C. (1999). Protein interactions with the glucose transporter binding protein GLUT1CBP that provide a link between GLUT1 and the cytoskeleton. *Mol. Biol. Cell* **10**, 819-832.
- Cai, H. and Reed, R. R. (1999). Cloning and characterization of neuropilin-1-interacting protein: a PSD-95/Dlg/ZO-1 domain-containing protein that interacts with the cytoplasmic domain of neuropilin-1. *Neuroscience* **91**, 6519-6527.
- Chinkers, M. and Garbers, D. L. (1989). The protein kinase domain of the ANP receptor is required for signaling. *Science* **245**, 1392-1394.
- Cho, J. Y., Chak, K., Andreone, B. J., Wooley, J. R. and Kolodkin, A. L. (2012). The extracellular matrix proteoglycan perlecan facilitates transmembrane semaphorin-mediated repulsive guidance. *Genes Dev.* **26**, 2222-2235.
- Davies, S. A. (2006). Signalling via cGMP: lessons from *Drosophila*. *Cell. Signal.* **18**, 409-421.
- De Vries, L., Lou, X., Zhao, G., Zheng, B. and Farquhar, M. G. (1998). GIPC, a PDZ domain containing protein, interacts specifically with the C terminus of RGS-GAIP. *Proc. Natl. Acad. Sci. USA* **95**, 12340-12345.
- Desai, C. J., Gindhart, J. G., Jr, Goldstein, L. S. and Zinn, K. (1996). Receptor tyrosine phosphatases are required for motor axon guidance in the *Drosophila* embryo. *Cell* **84**, 599-609.
- Dickson, B. J. (2002). Molecular mechanisms of axon guidance. *Science* **298**, 1959-1964.
- Djiane, A. and Mlodzik, M. (2010). The *Drosophila* GIPC homologue can modulate myosin based processes and planar cell polarity but is not essential for development. *PLoS ONE* **5**, e11228.
- Dontchev, V. D. and Letourneau, P. C. (2002). Nerve growth factor and semaphorin 3A signaling pathways interact in regulating sensory neuronal growth cone motility. *Neuroscience* **112**, 6659-6669.
- Gao, Y., Li, M., Chen, W. and Simons, M. (2000). Synectin, syndecan-4 cytoplasmic domain binding PDZ protein, inhibits cell migration. *J. Cell. Physiol.* **184**, 373-379.
- Gibbs, S. M., Becker, A., Hardy, R. W. and Truman, J. W. (2001). Soluble guanylate cyclase is required during development for visual system function in *Drosophila*. *Neuroscience* **107**, 7705-7714.
- Golemis, E. A., Gyuris, J. and Brent, R. (1994). Interaction trap/two hybrid system to identify interacting proteins. In *Current Protocols in Molecular Biology*, pp. 13.14.1-13.14.17. New York: Wiley.
- Grenningloh, G., Rehm, E. J. and Goodman, C. S. (1991). Genetic analysis of growth cone guidance in *Drosophila*: fasciclin II functions as a neuronal recognition molecule. *Cell* **67**, 45-57.
- Guo, D., Tan, Y. C., Wang, D., Madhusoodanan, K. S., Zheng, Y., Maack, T., Zhang, J. J. and Huang, X. Y. (2007). A Rac-cGMP signaling pathway. *Cell* **128**, 341-355.
- Guo, D., Zhang, J. J. and Huang, X. Y. (2010). A new Rac/PAK/GC/cGMP signaling pathway. *Mol. Cell. Biochem.* **334**, 99-103.
- Hidalgo, A. and Brand, A. H. (1997). Targeted neuronal ablation: the role of pioneer neurons in guidance and fasciculation in the CNS of *Drosophila*. *Development* **124**, 3253-3262.
- Hirakawa, T., Galet, C., Kishi, M. and Ascoli, M. (2003). GIPC binds to the human lutropin receptor (hLHR) through an unusual PDZ domain binding motif, and it regulates the sorting of the internalized human chorionic gonadotropin and the density of cell surface hLHR. *J. Biol. Chem.* **278**, 49348-49357.
- Hülsmeier, J., Pielage, J., Rickert, C., Technau, G. M., Klämbt, C. and Stork, T. (2007). Distinct functions of alpha-Spectrin and beta-Spectrin during axonal pathfinding. *Development* **134**, 713-722.
- Jeanneteau, F., Guillain, O., Diaz, J., Griffon, N. and Sokoloff, P. (2004). GIPC recruits GAIP (RGS19) to attenuate dopamine D2 receptor signaling. *Mol. Biol. Cell* **15**, 4926-4937.
- Jeong, S., Juhaszova, K. and Kolodkin, A. L. (2012). The Control of semaphorin-1a-mediated reverse signaling by opposing pebble and RhoGAPp190 functions in *Drosophila*. *Neuron* **76**, 721-734.
- Kedlaya, R. H., Bhat, K. M., Mitchell, J., Darnell, S. J. and Setaluri, V. (2006). TRP1 interacting PDZ-domain protein GIPC forms oligomers and is localized to intracellular vesicles in human melanocytes. *Arch. Biochem. Biophys.* **454**, 160-169.
- Kim, J., Lee, S., Ko, S. and Kim-Ha, J. (2010). dGIPC is required for the locomotive activity and longevity in *Drosophila*. *Biochem. Biophys. Res. Commun.* **402**, 565-570.
- Klaes, A., Menne, T., Stollewerk, A., Scholz, H., Klämbt, C. (1994). The Ets transcription factors encoded by the *Drosophila* gene pointed direct glial cell differentiation in the embryonic CNS. *Cell* **78**, 149-160.
- Kolodkin, A. L. and Tessier-Lavigne, M. (2011). Mechanisms and molecules of neuronal wiring: a primer. *Cold Spring Harb. Perspect. Biol.* **3**, a001727.
- Landgraf, M., Bossing, T., Technau, G. M. and Bate, M. (1997). The origin, location, and projections of the embryonic abdominal motoneurons of *Drosophila*. *Neuroscience* **77**, 9642-9655.
- Lin, D. M., Fetter, R. D., Kopczynski, C., Grenningloh, G. and Goodman, C. S. (1994). Genetic analysis of Fasciclin II in *Drosophila*: defasciculation, refasciculation, and altered fasciculation. *Neuron* **13**, 1055-1069.

- Lou, X., Yano, H., Lee, F., Chao, M. V. and Farquhar, M. G. (2001). GIPC and GAIP form a complex with TrkA: a putative link between G protein and receptor tyrosine kinase pathways. *Mol. Biol. Cell* **12**, 615-627.
- Mahr, A. and Aberle, H. (2006). The expression pattern of the Drosophila vesicular glutamate transporter: a marker protein for motoneurons and glutamatergic centers in the brain. *Gene Expr. Patterns* **6**, 299-309.
- Ming, G. L., Song, H. J., Berninger, B., Holt, C. E., Tessier-Lavigne, M. and Poo, M. M. (1997). cAMP-dependent growth cone guidance by netrin-1. *Neuron* **19**, 1225-1235.
- Mlodzik, M., Baker, N. E. and Rubin, G. M. (1990). Isolation and expression of scabrous, a gene regulating neurogenesis in Drosophila. *Genes Dev.* **4**, 1848-1861.
- Naccache, S. N., Hasson, T. and Horowitz, A. (2006). Binding of internalized receptors to the PDZ domain of GIPC/syneclin recruits myosin VI to endocytic vesicles. *Proc. Natl. Acad. Sci. USA* **103**, 12735-12740.
- Nishiyama, M., Hoshino, A., Tsai, L., Henley, J. R., Goshima, Y., Tessier-Lavigne, M., Poo, M. M. and Hong, K. (2003). Cyclic AMP/GMP-dependent modulation of Ca²⁺ channels sets the polarity of nerve growth-cone turning. *Nature* **423**, 990-995.
- Polleux, F., Morrow, T. and Ghosh, A. (2000). Semaphorin 3A is a chemoattractant for cortical apical dendrites. *Nature* **404**, 567-573.
- Potter, L. R. (2011). Guanylyl cyclase structure, function and regulation. *Cell. Signal.* **23**, 1921-1926.
- Ramadan, N., Flockhart, I., Booker, M., Perrimon, N. and Mathey-Prevot, B. (2007). Design and implementation of high-throughput RNAi screens in cultured Drosophila cells. *Nat. Protoc.* **2**, 2245-2264.
- Ranganayakulu, G., Schulz, R. A. and Olson, E. N. (1996). Wingless signaling induces nautilus expression in the ventral mesoderm of the Drosophila embryo. *Dev. Biol.* **176**, 143-148.
- Ruiz-Gómez, M., Coutts, N., Price, A., Taylor, M. V. and Bate, M. (2000). Drosophila dumbfounded: a myoblast attractant essential for fusion. *Cell* **102**, 189-198.
- Schmidt, H., Stonkute, A., Jüttner, R., Koesling, D., Friebe, A. and Rathjen, F. G. (2009). C-type natriuretic peptide (CNP) is a bifurcation factor for sensory neurons. *Proc. Natl. Acad. Sci. USA* **106**, 16847-16852.
- Schneider, I. (1972). Cell lines derived from late embryonic stages of Drosophila melanogaster. *J. Embryol. Exp. Morphol.* **27**, 353-365.
- Seidel, C. and Bicker, G. (2000). Nitric oxide and cGMP influence axonogenesis of antennal pioneer neurons. *Development* **127**, 4541-4549.
- Sepp, K. J., Schulte, J. and Auld, V. J. (2001). Peripheral glia direct axon guidance across the CNS/PNS transition zone. *Dev. Biol.* **238**, 47-63.
- Shelly, M., Lim, B. K., Cancedda, L., Heilshorn, S. C., Gao, H. and Poo, M. M. (2010). Local and long-range reciprocal regulation of cAMP and cGMP in axon/dendrite formation. *Science* **327**, 547-552.
- Song, H., Ming, G., He, Z., Lehmann, M., McKerracher, L., Tessier-Lavigne, M. and Poo, M. (1998). Conversion of neuronal growth cone responses from repulsion to attraction by cyclic nucleotides. *Science* **281**, 1515-1518.
- Tan, C., Deardorff, M. A., Saint-Jeannet, J. P., Yang, J., Arzoumanian, A. and Klein, P. S. (2001). Kermit, a frizzled interacting protein, regulates frizzled 3 signaling in neural crest development. *Development* **128**, 3665-3674.
- Terman, J. R., Mao, T., Pasterkamp, R. J., Yu, H. H. and Kolodkin, A. L. (2002). MICALs, a family of conserved flavoprotein oxidoreductases, function in plexin-mediated axonal repulsion. *Cell* **109**, 887-900.
- Thompson, D. K. and Garbers, D. L. (1995). Dominant negative mutations of the guanylyl cyclase-A receptor. Extracellular domain deletion and catalytic domain point mutations. *J. Biol. Chem.* **270**, 425-430.
- Togashi, K., von Schimmelmann, M. J., Nishiyama, M., Lim, C. S., Yoshida, N., Yun, B., Molday, R. S., Goshima, Y. and Hong, K. (2008). Cyclic GMP-gated CNG channels function in Sema3A-induced growth cone repulsion. *Neuron* **58**, 694-707.
- Van Vactor, D., Sink, H., Fambrough, D., Tsao, R. and Goodman, C. S. (1993). Genes that control neuromuscular specificity in Drosophila. *Cell* **73**, 1137-1153.
- Varsano, T., Dong, M. Q., Niesman, I., Gacula, H., Lou, X., Ma, T., Testa, J. R., Yates, J. R., III and Farquhar, M. G. (2006). GIPC is recruited by APPL to peripheral TrkA endosomes and regulates TrkA trafficking and signaling. *Mol. Cell. Biol.* **26**, 8942-8952.
- Wang, L. H., Kalb, R. G. and Strittmatter, S. M. (1999). A PDZ protein regulates the distribution of the transmembrane semaphorin, M-SemF. *J. Biol. Chem.* **274**, 14137-14146.
- Wills, Z., Bateman, J., Korey, C. A., Comer, A. and Van Vactor, D. (1999). The tyrosine kinase Abl and its substrate enabled collaborate with the receptor phosphatase Dlar to control motor axon guidance. *Neuron* **22**, 301-312.
- Winberg, M. L., Mitchell, K. J. and Goodman, C. S. (1998a). Genetic analysis of the mechanisms controlling target selection: complementary and combinatorial functions of netrins, semaphorins, and IgCAMs. *Cell* **93**, 581-591.
- Winberg, M. L., Noordermeer, J. N., Tamagnone, L., Comoglio, P. M., Spriggs, M. K., Tessier-Lavigne, M. and Goodman, C. S. (1998b). Plexin A is a neuronal semaphorin receptor that controls axon guidance. *Cell* **95**, 903-916.
- Yanagawa, S., Lee, J. S. and Ishimoto, A. (1998). Identification and characterization of a novel line of Drosophila Schneider S2 cells that respond to wingless signaling. *J. Biol. Chem.* **273**, 32353-32359.
- Yi, Z., Petralia, R. S., Fu, Z., Swanwick, C. C., Wang, Y. X., Prybylowski, K., Sans, N., Vicini, S. and Wenthold, R. J. (2007). The role of the PDZ protein GIPC in regulating NMDA receptor trafficking. *Neuroscience* **27**, 11663-11675.
- Yu, H. H., Araj, H. H., Ralls, S. A. and Kolodkin, A. L. (1998). The transmembrane Semaphorin Sema I is required in Drosophila for embryonic motor and CNS axon guidance. *Neuron* **20**, 207-220.
- Yu, H. H., Huang, A. S. and Kolodkin, A. L. (2000). Semaphorin-1a acts in concert with the cell adhesion molecules fasciclin II and connectin to regulate axon fasciculation in Drosophila. *Genetics* **156**, 723-731.
- Zhao, Z. and Ma, L. (2009). Regulation of axonal development by natriuretic peptide hormones. *Proc. Natl. Acad. Sci. USA* **106**, 18016-18021.

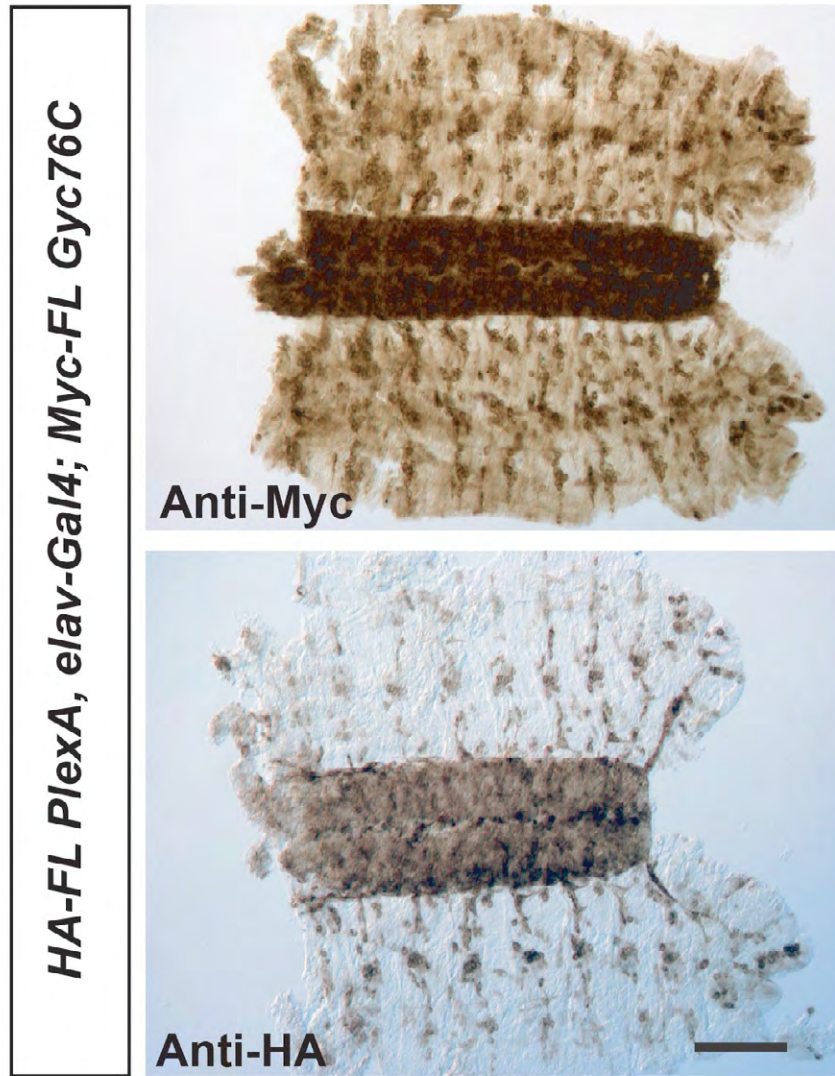


Fig. S1. Immunohistochemistry of *UAS:HA-FL PlexA, elav-Gal4; UAS:Myc-FL Gyc76C* embryos. Filleted stage 14-15 *UAS:HA-FL PlexA, elav-Gal4; UAS:Myc-FL Gyc76C* *Drosophila* embryos stained with anti-Myc (top panel) or anti- HA (bottom panel) reveal the neuronal expression of each transgene. Scale bar, 20 μ m.

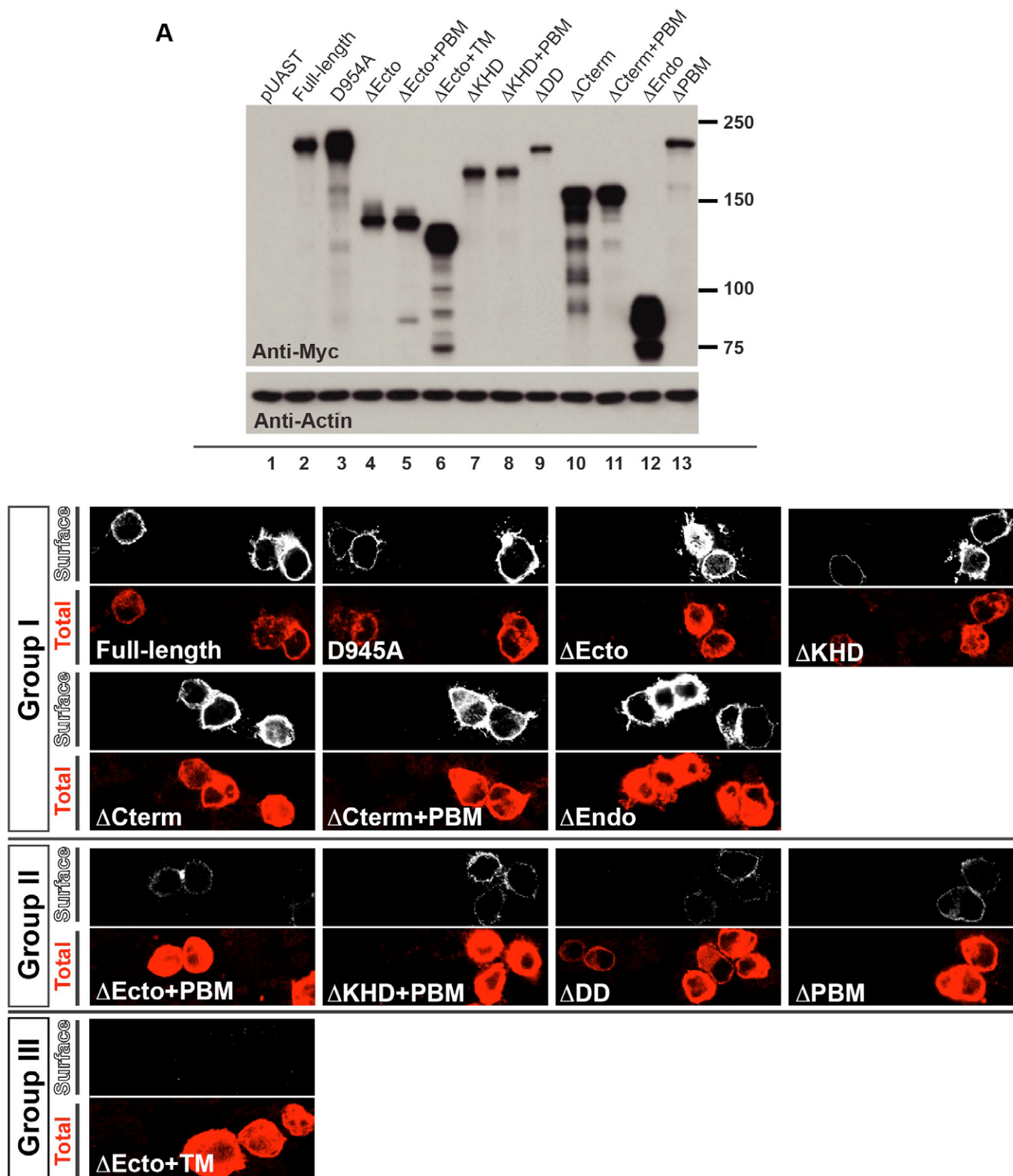
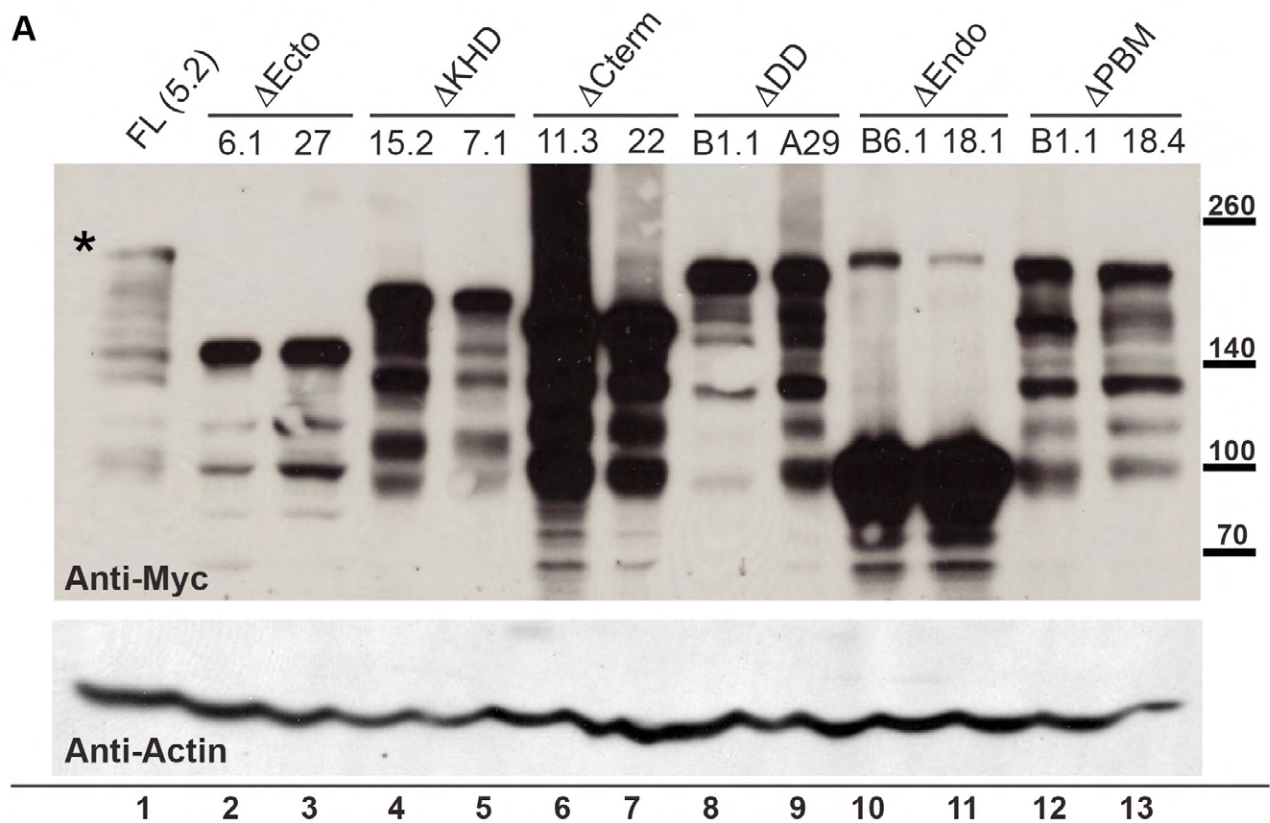


Fig S2. Western blot analysis and live cell-surface immunostaining reveal protein expression level and protein localization of Gyc76C constructs expressed in S2R+ cells under the control of *Actin-Gal4*. (A) Western analyses of lysates from *Drosophila* S2R+ cells used in cGMP assays. Cells were transfected with *Myc-FL Gyc76C*, or all *Myc-Gyc76C* deletion constructs described in the text, and then immunoblotted with anti-Myc (top panel). The control for protein loading was provided by immunoblotting for anti-actin (bottom panel). (B) Live cell-surface immunostaining using anti-Myc (9E10) was performed to label surface proteins (in white) of all *Myc-Gyc76C* constructs expressed in S2R+ cells prior to fixation and permeabilization. The total protein produced by each *Myc-Gyc76C* construct (in red; pseudo color) was observed by then labeling with rabbit anti-Myc (71D10) following fixation and permeabilization. The *Gyc76C* constructs in Group I (FL, ΔEcto, ΔKHD, ΔCterm, ΔCterm+PBM, and ΔEndo) show strong cell surface localization; those in Group II (ΔEcto+PBM, ΔKHD+PBM, ΔDD, and ΔPBM) show weak cell surface localization are; and (ΔEcto+TM) in Group III shows no cell surface protein localization.



Anti-MHC Anti-Sema-1a

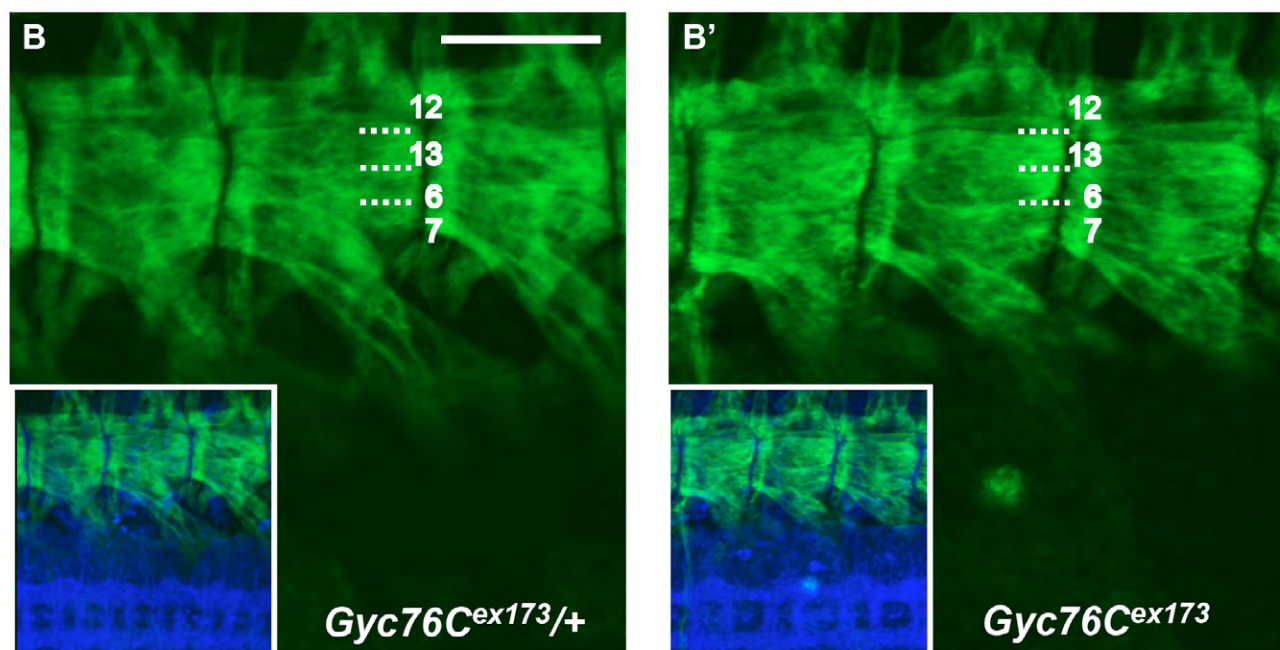


Fig. S3. Western blot analysis of *Gyc76C* transgene expression levels driven by *elav-Gal4*, and overall muscle development and organization of *Gyc76C* homozygous mutant embryos. (A) Equal amounts of embryonic lysates (1 embryo/4ul of Laemmli buffer) obtained from each transgenic line were subjected to Western analysis and blotting with anti-Myc (top panel). The loading control is provided by immunoblotting using anti-actin (bottom panel). (B) and B') Stage 16 embryos stained with anti-MHC and anti-Sema-1a (blue) to reveal overall ventro-lateral muscle field organization (green). *Gyc76C* heterozygous and *Gyc76C* homozygous embryos show no apparent differences in muscle development or organization. Scale bar, 10 μ m.

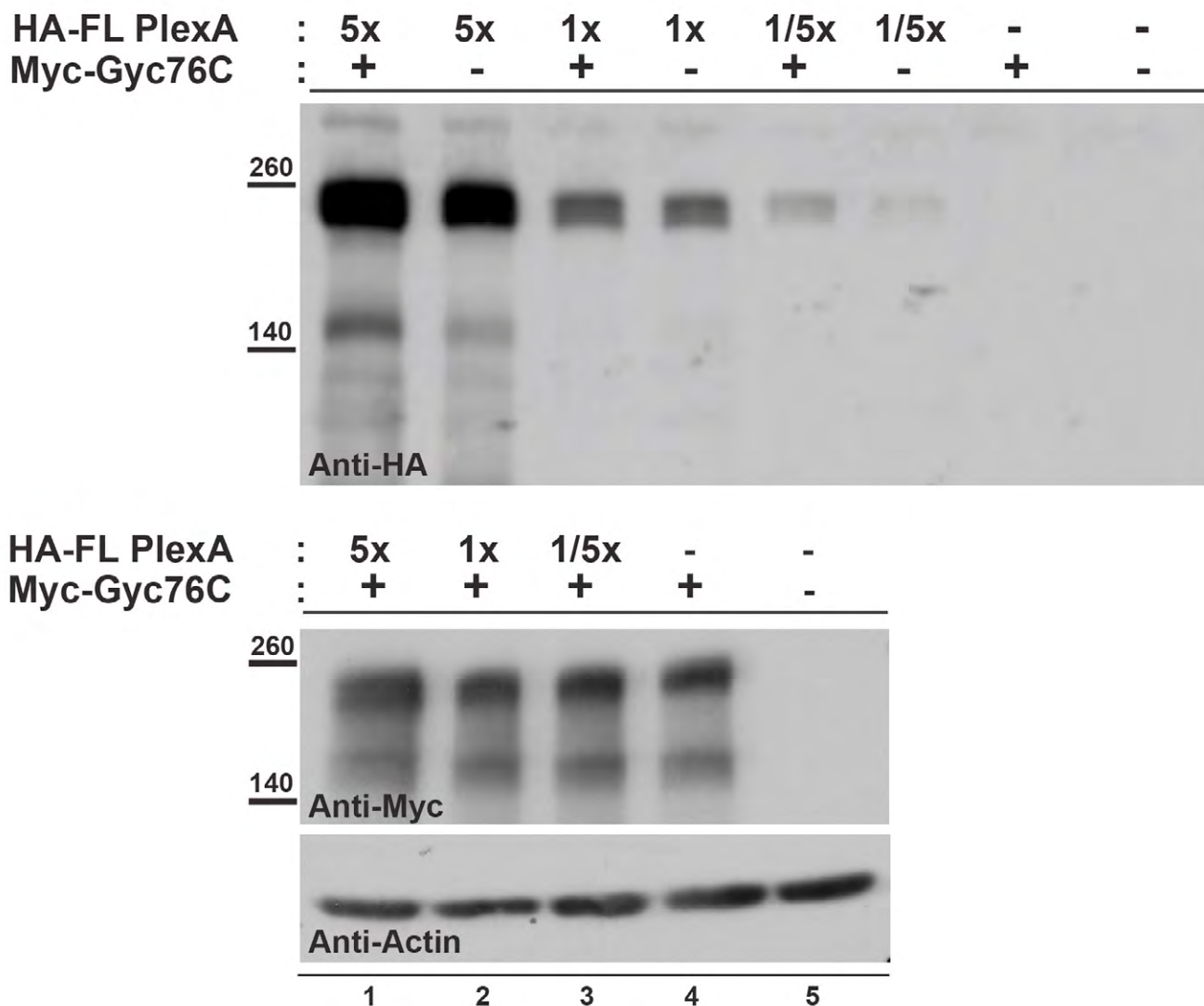


Fig. S4. Representative Western blots for PlexA: Gyc76C *in vitro* co-expression experiments used for GC assays. Lysates from Myc-FL Gyc76C-expressing DmBG2 cells with, or without, transfection using different amounts of HA-FL PlexA cDNA. Anti-HA and anti-Myc were used to detect HA-FL PlexA (top panel) and Myc-FL Gyc76C (middle panel), respectively. Different concentrations of HA-FL-PlexA did not influence the expression levels of Myc-FL Gyc76C (middle panel, lanes 1-4). The loading control was performed by immunoblotting using anti-actin (bottom panel).

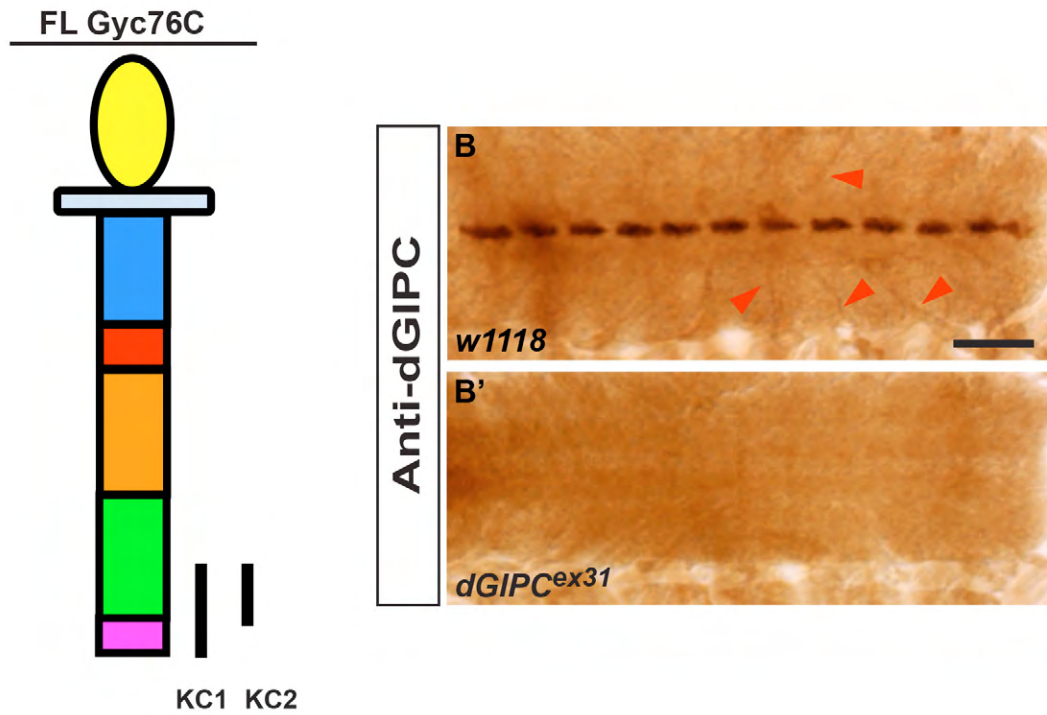


Fig. S5. Gyc76C baits for yeast-two-hybrid and endogenous dGIPC protein expression in the developing ventral nerve cord of *Drosophila* embryos. (A) Schematic diagram showing the protein landscape of Gyc76C that includes the PCR-amplified Gyc76C KC1 (aa 1451-1525) and KC2 (aa 1451-1522) fragments (black lines) used for constructing “baits” for yeast-two-hybrid assay. (B) and (B') Filleted preparations of wild-type and *dGIPC^{ex31}* stage 14 embryos stained with a mouse monoclonal antibody directed against dGIPC. (C) dGIPC protein is strongly expressed in midline glia but is also detected in other regions, including ventral nerve roots (red arrowheads). (C') dGIPC staining, including at ventral nerve roots, is absent in *dGIPC^{ex31}* null mutants. Scale bar, 10 μ m.